WYLE LABORATORIES - RESEARCH STAFF

REPORT NUMBER WR 66-46

PROGRAM TO MEASURE THE MACROSCALE TURBULENCE OF SUBSONIC JETS

Submitted Under Contract NAS 8-11312

Prepared by E. B. Miller

Approved by R. C. Potter
Program Manager

Prepared by R. C. Potter

Approved by L. C. Sutherland
Research Operations Manager

Date November 1966

COPY NO. 51

SUMMARY

The experiments reported here are to extend the description of a turbulent shear flow beyond the normally used statistical presentation. The use of many hot wire anemometers in an array allows the instantaneous pictures of turbulence to be formed. The data of all the matched channels must be acquired simultaneously and with the correct phase relationships. Eight hot wires, arranged as four cross-wire pairs, were used with a high speed analog-to-digital converter and a digital data acquisition system to study the macroscale of the turbulent shear region of several small subsonic cold air jets. A description of the apparatus is presented and the experimental techniques are described. The data analysis and presentation programs are described, and some preliminary results for presentation of the fluctuating velocity components are also given. Possible techniques for calculating the instantaneous vorticity components and transverse scale of the turbulence are given in the Appendices. It is concluded that a powerful method for turbulence analysis exists, which should help in the formation of turbulence models. These experiments are continuing.

TABLE OF CONTENTS

TABLE OF CONTENTS (Continued)

LIST OF FIGURES

LIST OF FIGURES (Continued)

LIST OF SYMBOLS

a	mole fraction of atmospheric gases (dimensionless)
c_0	velocity of sound under stagnation conditions (ft./second)
c_v	specific heat per mole at constant volume
C	mean vorticity vector (sec^{-1})
E	turbulence induced fluctuating anemometer output (volts)
E_m	anemometer output due to the mean velocity (volts)
E_0	anemometer output at zero velocity (volts)
G	arbitrary power spectral density parameter in plots of spectra
h	anemometer calibration constant (dimensionless)
H_R	relative humidity (dimensionless)
k	anemometer calibration constant, $[volt^2 \cdot (seconds/ft.)^h]$
$\underset{\sim}{L}$	a position vector having magnitude, L, (ft.)
M	the molecular mass of a single gas (atomic mass units expressed as slugs)
M_m	the molecular mass of a gas mixture (atomic mass units expressed as slugs)
O	the origin of a coordinate system
P	static pressure (inches of oil)
P_{atm}	atmospheric pressure (inches of mercury)
P_0	total pressure (inches of oil)
P_{SAT}	saturation vapor pressure for water vapor (atmospheres)
P_s	excess of static pressure above atmospheric pressure (inches oil)
P_t	excess of total pressure above atmospheric pressure (inches of oil)

P_v vapor pressure of water vapor (atmospheres)

R universal gas constant (4.972×10^4 lbf · ft./°Rankine)

T_0 stagnation temperature (°Rankine)

T_R arbitrary temperature (°Rankine)

u velocity component in the x-direction (ft./sec.)

U mean velocity in the jet flow (ft./sec.)

U_o velocity in the potential core of the jet (ft./sec.)

U_0 stagnation velocity and identically equal to zero by definition

v velocity component in the y-direction (ft./sec.)

w velocity component in the z-direction (ft./sec.)

x mole fraction of water vapor in atmosphere, section 3.3 only, (dimensionless)

x,y,z cartesian coordinates describing positions in the jet flow (ft.)

Greek Symbols

γ ratio of the specific heats of a gas (dimensionless)

γ_m ratio of the specific heats of a gas mixture (dimensionless)

$\underset{\sim}{\Gamma}$ the vorticity vector (sec^{-1})

ζ component of vorticity in z-direction (sec^{-1})

η component of vorticity in y-direction (sec^{-1})

θ orientation of hot film sensors, sections 4 through 5 and Appendix D, only (degrees)

θ velocity component in spherical polar coordinates (ft./sec.)

ξ component of vorticity in x-direction (sec^{-1})

ρ	velocity, component in spherical polar coordinates (ft./sec.)
ρ	density of air at static pressure under adiabatic conditions, sections 3.1 through 3.4 only, (slugs/ft.^{3})
ρ_0	density of air under stagnation conditions (slug/ft.^{3})
ρ_{HG}	density of mercury (gm/cm^3)
ρ_{oil}	density of oil (gm/cm^3)
ϕ	velocity component in spherical polar coordinates (radians)

1.0 INTRODUCTION

This report describes progress on a program designed to produce basic experimental results on the turbulent mixing of jet flows. A better understanding of the mixing process will help produce more complete ideas on the basic mechanism of aerodynamic noise generated by such turbulent shear flows. This will be of importance estimating exhaust noise of proposed space vehicles, and for determining optimum methods for reducing or controlling the acoustic pressure field generated at the test and launch stand.

The jet mixing region formed when a cold subsonic flow of gas mixes with a stationary atmosphere is shown in Figure 1. Here the three regions of the jet mixing are indicated. First, there is the initial mixing region, where the flow contains a laminar core of gas with an approximately uniform exit velocity. This is followed by a transition region where the near flow properties are changing to those of the fully developed region downstream. The initial and fully mixed regions are characterized by similar mean velocity profiles which can be normalized for all positions in the flow.

The initial theory of aerodynamic noise generation, due to Lighthill (Reference 1), was based on a complicated expression in terms of the correlation of the fluctuating velocity components in the flow. The use of this theory requires a detailed knowledge of the turbulent flow. The use of statistical descriptions of the flow enables certain values to be estimated, but an adequate theory for turbulent shear flows are still lacking. The major theoretical attack on free turbulence structure has concentrated on the simpler homogenous and isotropic flows, rather than the shear flows, and even here no exact theory is yet available. The basic problem can be traced to the very nature of the turbulence, in that it is a random and unpredictible motion. For this reason the statistical approach has been the most successful to date. This approach is based on defining the average values of the fluctuations in velocity and pressure, and, with the use of correlation techniques, allows the propagation at two different points to be related for a stationary process. As a result many experimental measurements have been made of jet mixing properties (References 2, 3, 4, and 5), and a fairly complete statistical description is now available. The normalized velocity profiles, intensity of turbulence in various directions, the normalized spectra of the fluctuating velocity and the eddy scales defined by the appropriate correlation curves have all been well documented. The normalized pressure fluctuation spectra has also been determined, for a limited range of turbulent shear flows, (References 5, 7, and 8).

Despite all these extensive experimental results, a detailed theory of turbulent mixing has not yet been put forward and fully substantiated by experimental measurements. The fact that the turbulent mixing is a real and constantly varying process means that the statistical descriptions of "eddies" are difficult to visualize as real fluid processes. Therefore, the objective of the experimental program

reported here was to extend the experimental knowledge of such flows to assist in developing theories of turbulent mixing and appropriate phenomenological models that could help provide a better understanding of the whole process.

The initial attempts for a turbulence theory start with the Prandtl mixing length theory (Reference 9). Although this theory contains assumptive errors, it does allow the general mixing of the jet to be determined, (References 10 and 11) Basically, the theory describes the turbulent reaction and its effects in terms of an appropriate length, scaled to the mean flow properties. The statistical theories which follow start from Taylor's work (Reference 12 and many others) which led to the work of Batchelor (Reference 13) and Townsend (Reference 14) on an homogenous and shear flow turbulence, respectively. The results that the reported experiments cover, represent an attempt to move one more step in the chain of descriptive process. The ultimate aim is to produce a complete experimental description of a piece of turbulent flow, with all the appropriate components listed with time, and not averaged. Then rather than describing a statistical eddy, the instantaneous flow of an actual turbulent eddy, will be measured and reproduced for analysis. This information will then be available for application to theoretical models of turbulent shear flows.

The measurement technique involved the simultaneous operation of eight constant-temperature hot-wire anemometers. At a latter date it is proposed to extend this number to give a more complete picture of the flow. The data acquired from these probes provide actual instantaneous values rather than statistical average results as obtained previously. The results can be used to visualize an isolated segment of turbulence, as the flow is convected past the probes. The measurement technique requires that the results be obtained with equal sensitivity between the various channels, so simultaneous results are obtained for each point where the probes are located. To achieve this, the analog equipment was kept to a minimum and the results recorded on real-time as digital values using the Wyle on-line digital data acquisition system. This comprises multiplexers, analog-to-digital converters, and a CDC 3300 computer. The apparatus and recording system are described in detail in the next chapter of this report. Once the data has been acquired and stored on tape in a digital form, it can be manipulated and analyzed to produce the required results without sacrificing any details or calibration of the eight channels. The elimination of an analog tape recorder and the errors introduced by repeated play-back of tape loops ensures that the required accuracy and absolute values of the data are maintained.

This report is the first report issued on this work, and, as such, is concerned with descriptions of the apparatus, the techniques used, and the details of the analysis programs. The detailed descriptions of the turbulence obtained and the pictures of turbulence measured will be presented in latter reports. The initial measurements and some selected results are presented however, and they indicated the power of this approach in studying turbulence. As mentioned before it is hoped to extend the system to include many more simultaneous measurements.

2.0 DESCRIPTION OF APPARATUS

The turbulence measurements were made in the exhaust flow of three different size jets blowing unheated air. The flow system incorporated a small blower, a muffler, and a settling tank. The hot-wire anemometers used were Thermo-Systems Model Constant Temperature Hot-Wire Anemometers. They were generally operated as 4 probes each with 2 crossed wire elements. After the mean voltage output of the anemometer amplifiers was removed, the signals were acquired directly by the digital data acquisition system.

2.1 Blower Systems

A centrifugal blower was used to supply the air. The apparatus was set up in a closed room, where the ambient air was cooled and maintained clean by the normal commercial air conditioning system. The air from the jets was recirculated in the room, and the problem of water vapor and dirt in the supply system eliminated. The airflow supplied to the jet was controlled by a butterfly valve, a baffle on the blower intake, and a door on the blower casing. Figure 2 shows the blower and these control devices. By setting the intake baffle and the casing door at various positions, very fine control of the airflow, over a wide range of deliveries, was possible using the butterfly valve. To reduce vibration effects the blower was isolated from a muffler by a short length of 12 in. diameter flexible hose and it was also mounted on isolation pads. The muffler was a simple glass fiber absorption device, designed to remove the blower noise from the airflow.

2.2 Settling Tank and Nozzles

A settling tank, 6 ft. in length, was attached to the muffler. The combined length including the muffler was 14 ft. and the internal diameter was 10 inches throughout. A series of 7 screens of mesh size reducing to 50 holes per linear inch were fixed in the settling tank by spot welding. This gave a very smooth flow to the nozzles. Figure 3 is a general view of the rig and shows the settling tank.

The nozzle exit diameters were 4.0, 2.5, and 1.0 inches, respectively. The contractions were chosen to give an even airflow with no separation, and were designed on a one dimensional analysis of the cross-sectional area. The nozzles are shown in Figure 4 with their relevant dimensions. They were made from fiberglass on a turned wooden mold. This technique allows complicated shapes to be made accurately with a smooth finish, but without the machining problems of metal nozzles. The nozzles incorporate a short parallel entrance and exit section to achieve the optimum result of an even laminar exit velocity, with minimum boundary layer effects to increase the initial mixing region width.

2.3 Mean Flow Parameter Measuring Instruments

The mean velocity profiles of the jet were measured using two pitot-static combinations. These are shown in Figure 5. Here a simple combination is shown at the center, the diameter of this tube was 0.07 inch. At the top is shown a combined pitot tube and thermocouple for measuring the mean temperature and velocity of the flow. The copper-constantan thermocouple is mounted in a cavity open to the stream direction. The block also holds the pitot tube, so that the two measurements are obtained at essentially the same point. The final item at the bottom of Figure 5 is a total temperature thermocouple used with the simple pitot tube.

The pitot-static tubes were operated in conjunction with oil u-tube manometers and a Hook Gauge for measurements at very low pressures. This gauge can be seen in Figure 3 in the foreground near the probe holders. The thermo-couples were used with a Leeds and Northrop Temperature Potentiometer. This system was accurate to $\pm 0.5^{\circ}F$ for the range used.

These instruments enable the total and static pressures and mean temperature of the flow to be obtained throughout the mixing region. The mean velocity profiles were then calculated as explained in the next chapter.

2.4 Fluctuating Velocity Measurements

The fluctuating velocity components were measured using Thermo-System Model 1030 Constant Temperature Hot Wire Anemometers. The power supply and the eight amplifiers are shown mounted in the equipment rack in Figure 3. The probes are formed as a 0.060 inch long platinum film on a quartz rod 0.001 inch in diameter. This element is larger than the fine wires normally used in turbulence work, but the advantage of physical strength was more appealing since a total of eight wires had to be operated simultaneously. The frequency response of the Thermo-Systems Model 1030 system is limited to an upper frequency of 3000 Hz.. Because of the relatively large probes and this low frequency response, the measurements are limited to the macroscale of turbulence. This system matches the digital data acquisition system well, in that it can only acquire eight channels up to this frequency. This matter of system frequency response will be considered again in the section on digital data acquisition.

The wires were arranged in cross-pairs on 4 probes. Each pair then gave a measure of two velocity components. When the 4 probes are mounted close together, and oriented in the usual fashion in the mean flow direction the probes interfer with each other so that they give a measure of the fluctuating components in the mean flow direction and only one transverse direction. The actual probe arrangement used is shown in Figure 6, and magnified in Figure 7. This basic arrangement puts each set of wires at the corners of a square. The square is set at 45 degrees to the system axis defined by the individual probe traverse gear. In this arrangement the complete

system gives 4 measurements of the velocity fluctuations in the mean flow direction, and by suitably orientating the pairs of wires, 2 measurements of each of the 2 transverse axes velocity fluctuations. Figure 5 shows how the probe bodies were bound together once they had been placed in position. Figure 7 shows the sensor elements, and some of the wires can be seen. These probes were manufactured commercially to Wyle Laboratories specification. They are equipped with a shield tube, which slides forward over the elements for protection, when the anemometers are not in use.

As can be seen in Figure 6, the whole probe assembly can be traversed across the jet exit, and it could also be moved up and downstream relative to the jet axis by another screw thread transverse mechanism. The basic wire mounting ring is also used to hold the combined pitot tube and thermocouple for mean flow parameter measurements. It fits on to any of the four individual probe transverse mechanisms.

The second arrangement for the 4 hot wire anemometer probes is shown in Figure 8. Here the four probes are mounted on an airfoil, and are positioned to be on a horizontal traverse across the jet. The airfoil is shown dismantled in Figure 9, to indicate the construction. The four probes could be set at various spacings and oriented to measure either 4 transverse velocity components in the same axis, or 2 components in two axes. Normally all 4 probes were setup to measure the same transverse velocity component.

A three wire probe was also obtained, comprising 3 wires set at 90 degrees to each other, and arranged so each makes an equal angle to the mean flow. This probe (Figure 10) was to be used to measure the three fluctuating velocity components at a single point. One test proposed was to compare the usefulness of operating a series of such probes in place of an array of the two wire probes.

2.5 Data Acquisition and Reduction

The full system is shown in block diagram in Figure 11. The outputs of the eight wire anemometer amplifiers were fed to high pass filter circuits to eliminate any dc voltage input to the digital data system. This ensured that only the fluctuating component of the voltage was recorded, allowing the maximum sensitivity. A circuit diagram of two such channels is shown in Figure 12. The system was monitored with a cathode ray oscilloscope, and the RMS value and dc voltage of the signal measured by the appropriate meters. The dc voltage was measured to within $\pm$ 2 percent for the calibration of the wires in the steady airflow of the laminar core of the jet. Also, during each run, the dc voltage was recorded to allow the sensitivity of the non-linear wire system to be calculated as explained in chapter 3.

The CDC 3300 digital data acquisition system comprises two basic channels that could be multiplexed to take up to 128 channels each and timed together. The maximum sampling rate of each channel is 50,000 samples per second. As used here, each basic channel carried 4 signals, and the maximum sampling rate was used. This gives a sampling of 12,500 values per second on each channel. With an empirical figure of 5 samples per cycle necessary for a full determination of random data, the system was therefore capable of analysis up to 2500 Hz. Because of this high frequency limitation, the analysis is restricted to study of the macroscale of turbulence. The frequency limitation enabled a small inexpensive constant temperature anemometer system to be used. This is particularly advantageous since many channels must be examined.

Due to the physical problem of putting the probes close together, the smallest variations in velocity fluctuation in space cannot be covered. Therefore, the physical characteristics of the probes and the frequency limitation on the hot wire anemometers and the data acquisition system combine to produce a consistent piece of apparatus.

The analysis is completely digital, and therefore the problems of matching the channels and retaining data are eliminated. The detailed analysis programs developed so far are listed in Appendix B. The plotter, presenting visual records, was especially useful and various schemes for data presentation were tried. The initial programs were concerned with optimizing the calibration procedure, and calculating the individual velocity components. An initial presentation program was developed to attempt to represent the turbulence in a three dimensional manner.

3.0 MEAN VELOCITY DETERMINATION

The basic equations used to determine the mean velocities in the jet mixing region, from the measured data of the pitot-static combination and the thermocouple measurements, are presented in this chapter. Symbols employed are defined in the front of the report.

3.1 Basic Theory

For steady flow lacking vorticity, the velocity and pressure along a streamline are related by the differential form of the Bernoulli equation,

$$U\,dU + \frac{dP}{\rho} = 0 \tag{3.1}$$

The adiabatic relationship between pressure and density is,

$$\rho = \rho_0 \left[\frac{P}{P_0}\right]^{1/\gamma} \tag{3.2}$$

Substituting this equation into Equation 3a gives,

$$\int_{U_0}^{U} U\,dU + \frac{P_0^{\frac{1}{\gamma}}}{\rho_0} \int_{P_0}^{P} \frac{dP}{P^{1/\gamma}} = 0, \tag{3.3}$$

from which the Saint-Venant and Wantzel equation may be obtained, which is,

$$U^2 - U_0^2 = \frac{2\gamma}{\gamma-1} \frac{P_0}{\rho_0} \left[1 - \left(\frac{P}{P_0}\right)^{\frac{\gamma-1}{\gamma}}\right] \tag{3.4}$$

This equation is valid for compressible gases in accordance with the adiabatic relationship, Equation 3.2. Air obeys Equation 3.2 very well at the temperatures and pressures which characterize the experimental work described in this report.

The significance of the Saint-Venant and Wantzel Equation 3.4 and its relationship to the more elementary physical case of incompressible fluids can be seen by writing Equation 3.4 in the form,

$$\frac{P}{P_0} = \left[1 - \frac{(\gamma-1)(U^2 - U_0^2)\,\rho_0}{2\gamma\,P_0}\right]^{\frac{\gamma}{\gamma-1}} \tag{3.5}$$

and simplifying it in the following manner.

Using a common approximation and imposing the condition that $(U^2 - U_0^2) / c_0^2 \ll 1$, where c_0 is the velocity of sound and is related to P_0 and ρ_0 by

$$c_0^2 = \frac{\gamma P_0}{\rho_0} \quad , \tag{3.6}$$

produced the relationship,

$$\frac{P}{P_0} = \left[1 - \frac{\rho_0 (U^2 - U_0^2)}{2 P_0}\right] \quad . \tag{3.7}$$

This expression is valid only under the condition imposed above. Imposing this condition should make it possible to obtain the incompressible Bernoulli equation, since, at low Mach numbers, compressible fluids are known to obey equations for incompressible fluids.

Simplifying Equation 3.7 and remembering that for the incompressible case, $\rho_0 = \rho$, produces the expected result. The Bernoulli equation for the incompressible case is

$$P_0 = P + \frac{\rho U^2}{2} \quad , \tag{3.8}$$

where the 0 subscript has been chosen to designate the stagnation properties and the terms lacking a subscript are static properties. Obviously U_0 dissappears, since the velocity at a stagnation point is zero by definition. Equation 3.4 was used to measure the mean velocities in the jets, with a slight modification arising from the ideal gas low. Equation 3.4 may be written,

$$U^2 = \frac{2\gamma}{\gamma - 1} \frac{R T_0}{M} \left[1 - \left(\frac{P}{P_0}\right)^{\frac{\gamma - 1}{\gamma}}\right] \tag{3.9}$$

Thus, the quantities which are measured in order to calculate the velocity are the stagnation temperature, T_0, the stagnation pressure, P_0, and the static pressure, P. The pitot-static tube and specially mounted thermocouple or thermometer described earlier were used to make these measurements. Slight corrections were made to Equation 3.9 to allow for significant changes in humidity and temperature which could occur. In most cases these corrections are negligible. However, they

do assure more consistent data over a wide range of operating conditions.

3.2 Temperature Corrections

Pressure measurements were made using manometers referenced to atmospheric pressure and filled with a manometer oil for which a density versus temperature plot was furnished by the manufacturer. Atmospheric pressure was measured with a mercury manometer and a density versus temperature plot was obtained from Reference 15. The mercury manometer was located in a room which was generally at a different temperature than the room in which the oil manometers were located. Therefore corrections were necessary to make all manometer readings consistent.

The density - temperature relationships are linear and were fitted accurately by linear functions.

These functions are valid within the range 60° - 130° F. They give the densities of mercury and the manometer oil (Meriam D-2673 red oil) as a function of temperature in degrees Rankine. These expressions are,

$$\rho_{HG} = -\left[1.355\ (10)^{-3}\right]T_R + 14.262 \qquad (3.10a)$$

and

$$\rho_{oil} = -\left[3.773\ (10)^{-4}\right]T_R + 1.0229 \qquad (3.10b)$$

, where ρ_{HG} and ρ_{oil} are in gms/cm^3.

The relationships used for correcting the pressure measurements for the difference between measurement locations are

$$P = P_s + \frac{\rho_{HG}}{\rho_{oil}} \cdot Patm \qquad (3.11a)$$

and

$$P_0 = P_t + \frac{\rho_{HG}}{\rho_{oil}} \cdot Patm, \qquad (3.11b)$$

where ρ_{HG} and ρ_{oil} are evaluated at their respective temperatures. P_s and P_t are in inches of oil and are referenced to atmospheric pressure. Patm is atmospheric

pressure in inches of mercury. P and P_0 occur in a ratio in the Saint-Venant and Wantzel equation, Equation 3.4.

3.3 Humidity Corrections

Humidity effects enter Equation 3.4 through the molecular mass, M, and the specific heat ratio, γ. Changes in humidity result in changes in molecular mass and specific heat ratio through the change in the mole fractions of the constituents of air.

An expression which describes the dependence of the molecular mass on mole fractions of the constituents of an ideal gas mixture is,

$$M_m = \sum_{i=1}^{n} M_i \, a_i \, , \tag{3.12}$$

If we let the mole fraction of water vapor in the atmosphere be represented by the symbol x, and consider the four major gases comprising sea-level composition for a dry atmosphere given in Reference 16.

Constituent Gas	Mole Fraction	Molecular Mass
Nitrogen (N_2)	.7809	28.016
Oxygen (O_2)	.2095	32.000
Argon (A)	.0093	39.944
Carbon Dioxide (CO_2)	.0003	44.010
Water (H_2O)	x	18.016

then equation for the molecular mass of a humid atmosphere in terms of the variable x may be written as,

$$M_m = \left[M_{N_2} a_{N_2} + M_{O_2} a_{O_2} + M_A a_A + M_{CO_2} a_{CO_2}\right](1-x) + x M_{H_2O} \tag{3.13}$$

A similar expression may be derived for the ratio of the specific heats, γ. Using the following equations for ideal gases, it is possible to develop an expression for determining the ratio of the specific heats of the mixture in terms of the mixture constituents and the variable x.

$$c_{v_m} = \sum_{i=1}^{n} c_{v_i} a_i \tag{3.14}$$

$$1 = \sum_{i=1}^{n} a_i \tag{3.15}$$

$$c_v = \frac{R}{\gamma - 1} \tag{3.16}$$

This equation is,

$$\gamma_m = 1 + \left[\left(\frac{a_{N_2}}{\gamma_{N_2} - 1} + \frac{a_{O_2}}{\gamma_{O_2} - 1} + \frac{a_A}{\gamma_A - 1} + \frac{a_{CO_2}}{\gamma_{CO_2} - 1}\right)(1 - x) + \frac{x}{\gamma_{H_2O} - 1}\right]^{-1} \tag{3.17}$$

The problem now remains to interpret x in terms of the relative humidity H_R which is easily measured by a psychrometer. The relative humidity is defined as the ratio of the actual vapor pressure, P_v, to the pressure occurring at saturation, P_{SAT}.

$$H_R = \frac{P_v}{P_{SAT}} \tag{3.18}$$

From the law of partial pressures and the ideal gas law it is possible to show that, in general,

$$a_i = \frac{P_i}{P_m}, \tag{3.19}$$

or in the case of water vapor,

$$x = (29.92)\ \frac{P_v}{P_{atm}} \tag{3.20}$$

Thus considering Equations 3.18 and 3.20

$$x = (29.92)\ \frac{H_R\, P_{SAT}}{P_{atm}} \tag{3.21}$$

It was useful in programing this humidity correction to curve fit P_{SAT} versus temperature and two γ versus temperature relationships over the temperature range of 60° F to 130° F. The other γ values can be taken as constant with temperature over this range. All data were obtained from Reference 17. The expression for P_{SAT} in atmospheres as a function of the temperature in degrees Rankine is,

$$P_{SAT} = \left[1.714\ (10)^{-5}\right] T_R^2 - \left[1.735\ (10)^{-2}\right] T_R + (4.4068) \qquad (3.22)$$

over the given temperature range.

The values and functions for γ which were used in this humidity correction are,

$$\begin{aligned} \gamma_{H_2O} &= 1.30, \\ \gamma_{A} &= 1.67, \\ \gamma_{N_2} &= 1.40, \end{aligned} \qquad (3.23)$$

$$\gamma_{O_2} = -\left[4.386\ (10)^{-8}\right] T_R^2 + \left[4.4585\ (10)^{-5}\right] T_R + (1.3887)$$

and

$$\gamma_{CO_2} = -\left[8.7217\ (10)^{-9}\right] T_R^3 + \left[1.4518\ (10)^{-5}\right] T_R^2 - \left[8.4119\ (10)^{-3}\right] T_R + (2.9773)$$

where T_R is in degrees Rankine.

The effects of the corrections in Equation 3.13 and 3.17 on the Saint-Venant and Wantzel Equation 3.4 are to decrease the calculated value of the velocity slightly with increasing humidity at constant temperature. The effect may be neglected at moderate temperatures and high subsonic velocities. This decrease in the calculated value of the velocity could exceed 1%, however, under extreme conditions of humidity and temperature and at a low velocity.

Values of Velocity Calculated For
Saturated and Unsaturated Case at About 80° F.

Saturated ($H_R = 1.0$)	Unsaturated ($H_R = 0$)
95.38	95.45
104.5	104.5
114.7	114.8
138.5	138.7
158.2	158.4
175.2	175.5
180.7	181.1

3.4 Determining the Mean Velocity Distribution in the Jets

Three nozzles were used in acquiring data. The dimensions are shown in Figure 4. The jets were operated at a number of velocities between 150 fps and 300 fps for the purposes of determining the mean velocity profiles. These profiles were determined horizontally and vertically across the jet at two or more points in the flow to ascertain the flow center prior to investigations of the random velocity fluctuations. Figure 13 shows results of horizontal traverses of the jets. The axial distance from the jet and the horizontal distance, across the jet have been normalized to the jet diameter in each case and the maximum velocity for each profile has been normalized to the velocity in the potential core. As can be seen, all the jets show good symmetry properties and apparently differ very little when shown on the same normalized scale.

Program "POS" was developed to determine mean velocities in the jet, from the measured pitot-static pressures and the nozzle temperatures. Since the primary function of this program was to determine the center of the flow field, humidity corrections were not considered in calculating the profiles in Figure 13, temperature corrections were retained, however. A Fortran statement of this program is given in Appendix B.

4.0 FLUCTUATING VELOCITY MEASUREMENTS

4.1 Determination of the Fluctuating Velocity Components

Experimental work with hot film and hot wire anenometers has shown that for constant temperature operation a useful relation between velocity and voltage for a skewed wire or a cylindrical film is,

$$(E_m^2 - E_0^2) = k\ (U \sin\theta)^h \ , \tag{4.1}$$

where k and h are constants, E_0 is the voltage at zero velocity and E_m is an average voltage corresponding to a steady flow velocity. θ is the angle which the wire makes with the mean velocity vector.

The evaluation of k and h can be accomplished graphically or analytically by writing Equation 4.1 in the form,

$$\ell n\ (E_m^2 - E_0^2) = \ell n\ k + h\ \ell n\ (U \sin\theta). \tag{4.2}$$

The quantities $\ell n\ (E_m^2 - E_0^2)$ and $\ell n\ (U \sin\theta)$ are linearly related and the slope of a plot of these values determines h while the intercept for $\ell n\ (U \sin\theta) = 0$ determines k. Thus,

$$k = e^{\left[\ell n\ (E_m^2 - E_0^2)\right]} \quad \text{at } U \sin\theta = 0 \tag{4.3}$$

and

$$h = \frac{\left[\ell n\ (E_m^2 - E_0^2)\right]_1 - \left[\ell n\ (E_m^2 - E_0^2)\right]_2}{\left[\ell n\ (U \sin\theta)\right]_1 - \left[\ell n\ (U \sin\theta)\right]_2} \tag{4.4}$$

where 1 and 2 are representative points on the curve of $\ell n\ (E_m^2 - E_0^2)$ versus $\ell n\ (U \sin\theta)$.

The turbulent fluctuations observed in this experimental work produce a signal which is small compared with that produced by the mean flow velocity. These fluctuations are assumed in the data analysis to obey Equation 4.1 which is strictly true only for slowly varying velocities. Since this report deals with the macroscale

of turbulence the assumption is well justified. Frequencies exceeding 2500 Hz. were not observed in any data collected thus far.

Considering the small turbulence-induced fluctuating signal, E, about the mean voltage, $(E_m - E_0)$, and assuming the fluctuations are small enough to follow an approximately linear relationship to the velocity about the point $(E_m - E_0)$ allows one to write

$$E = \frac{\partial (E_m - E_0)}{\partial (U \sin \theta)} \left[u \sin \theta + v \cos \theta \right] \tag{4.5}$$

where u and v are the two fluctuating components of velocity in the mean flow direction and perpendicular to the mean flow direction respectively. The perpendicular component lies in the plane determined by the mean velocity vector, U, and the wire. Reference 18 demonstrates that these two components have the primary influence on the fluctuating signal from the hot film sensor. In short, a skewed hot film sensor is regarded in this analysis as only being sensitive to the normal components of the velocity fluctuations which lie in a plane determined by the mean flow direction and the very small diameter rod on which the film is deposited.

Coordinate axes will be chosen so that x is parallel to the axis of the jet and positive in the downstream direction, y is horizontal and positive to the left as one faces into the jet, and z is vertical and positive upwards. Fluctuating velocity components, u, v and w, correspond to x, y and z respectively.

Equation 4.1 may be applied to two hot film sensors making equal and opposite angles with the mean flow direction and in two closely spaced parallel planes, each determined by a sensor rod and the flow direction. In this case, two simultaneous equations are produced by which u and v or u and w may be determined.

Defining the sensitivity S, by the relation

$$S = \frac{\partial (E_m - E_0)}{\partial U \sin \theta} \tag{4.6}$$

permits the following two equations for sensors 1 and 2 on a given probe to be written.

$$\begin{aligned} E_1 &= S_1 \left[u \sin \theta + v \cos \theta \right] \\ E_2 &= S_2 \left[u \sin \theta - v \cos \theta \right] \end{aligned} \tag{4.7}$$

The velocity components u and v can then be determined from the expressions,

$$u = \left[\frac{E_1}{S_1} + \frac{E_2}{S_2}\right] \left[\frac{1}{2 \sin\theta}\right]$$

and

$$v = \left[\frac{E_1}{S_1} - \frac{E_2}{S_2}\right] \left[\frac{1}{2 \cos\theta}\right] \qquad (4.8)$$

The same analysis obviously applies to sensors which are arranged so as to be sensitive to the components of u and w.

4.2 Determining Sensitivity from Calibration Data

It is a simple matter to determine the sensitivity as a function of the mean voltage if the probe is calibrated so that h and k may be determined from the data by the method discussed in the previous section.

Differentiating $(E_m^2 - E_0^2)$ by $(U \sin\theta)$ in Equation 4.1 yields

$$\frac{\partial (E_m^2 - E_0^2)}{\partial (U \sin\theta)} = hk (U \sin\theta)^{h-1} \qquad (4.9)$$

Writing $(E_m^2 - E_0^2)$ as a function of $(E_m - E_0)$ and E_0 produces the equation,

$$(E_m^2 - E_0^2) = (E_m - E_0)^2 + 2 E_0 (E_m - E_0) \qquad (4.10)$$

Therefore,

$$\frac{1}{2}\left[(E_m^2 - E_0^2) + E_0^2\right]^{-1/2} \frac{\partial (E_m^2 - E_0^2)}{\partial (U \sin\theta)} = \frac{\partial (E_m - E_0)}{\partial (U \sin\theta)} \qquad (4.11)$$

Using Equations 4.1, 4.9 and 4.11 produces the final relation,

$$\frac{\partial (E_m - E_0)}{\partial (U \sin\theta)} = \frac{h (k)^{1/h} (E_m^2 - E_0^2)^{\frac{h-1}{h}}}{2\left[(E_m^2 - E_0^2) + E_0^2\right]^{1/2}} \qquad (4.12)$$

which makes possible the use of the mean output voltage and the calibration constants in determining the sensitivity of a hot film sensor.

5.0 COMPUTER PROGRAM TECHNIQUE

Two multiplexers, each capable of handling 4 channels of analog data are used in acquiring data from the anemometer system. Each multiplexer takes 50,000 samples per second so that the sampling rate per channel of data is 12,500 samples per second.

If the data channels are numbered 1 to 8, then channels 1 and 5 are sampled first followed by channels 2 and 6, 3 and 7, and 4 and 8, respectively. The sampled voltages from channels 1 and 5 are stored as one digital word on the tape followed by a word giving the voltages on 2 and 6, 3 and 7, etc., in a cyclic manner. To recover the data, the tape is "split" by a special program which properly groups and sequences the data for channels 1 to 8.

Because all channels are not sampled simultaneously, a question arises concerning the need of interpolating to determine the most probable points on all eight channels at any instant. So far, the frequencies measured have not exceeded 2500 Hz. This means that in the very worst case, there are 5 samples per cycle on each channel. Further, the initial data presentation programs are only considering every fifth data value. For these reasons, interpolation has not yet been attempted, however, routines are being prepared to interpolate when the frequency spectra indicate the necessity of doing so.

A computer program has been developed, and is presently being improved, which provides calibration curves and constants for eight hot film sensors. This program uses a method of least squares to fit a curve of $\ell n\ (U \sin \theta)$ versus $\ell n\ (E_m^2 - E_0^2)$ to the data. It then determines the slope, h, and the intercept, k, of this curve as discussed in chapter 4. These values are used in conjunction with measurements made during each data acquisition to determine the appropriate sensitivity for each hot film sensor. A routine has been successfully developed to determine the velocity components, u, v, and u, w from the appropriate sets of crossed wires. These velocity components in a cartesian coordinate system are also converted to velocity components in a spherical polar coordinate system by this program. Working under the assumption that the four probes are essentially at a point compared to the size of the large turbulent eddies, the program has been designed initially to take the ensemble average over all sets of sensors. This is an average of four values of u, two of v, and two of w. The results are then printed out.

A plotter program has also been developed, and is functioning properly. This program takes components of u, v, and w, and plots the associated vector at consecutive points along the u axis. The spacing between two points corresponds to the minimum time interval between samples multiplied by a scaling factor. The plot is isometric, with the w axis projecting apparently out of the paper, the v axis upward, and the u axis in the same direction as the time axis. At present no provision has been made to identify the quadrant in which the vector lies, although

this may be added later. Preliminary plots using several channels of data from the anemometer probes indicate that the plot will be extremely useful in visually assessing vortex motion in the flow.

6.0 PROGRAM OF MEASUREMENTS

A series of experiments were made, utilizing the three nozzles, with measurements made at various jet speeds and locations in the mixing flow. Two basic probe arrays were used. The majority of the measurements were made using a square array, with the probes arranged as shown in Figure 14. Here the probes are set in pairs in the transverse axis, and each probe gives a measure of the velocity fluctuations in the longitudinal direction and in one transverse direction. Probes 1 and 3 of Figure 14a measure the u and v fluctuating velocity components and Probes 2 and 4 measure the u and w fluctuating velocity components, after the voltage outputs have been added and subtracted as explained in chapter 4. The second array used was a line array, shown in Figure 14b, with the four probes set across the jet on the y axis. This layout was first used to measure 4 values of each of the u and v velocity components, and then the probes were rotated 90 degrees, about the probe body axis, to measure 4 values of the u and w velocity components.

The experimental procedure of Appendix A was followed for each run, and the signals were acquired as digital data by the computer acquisition system. Table I is a list of all the runs made, the raw data being available for later analysis. Each nozzle was operated at three jet exit velocities with the square probe arrangement. The 4 inch diameter nozzle was run at very low exit velocities. Because of the relatively large exit area of this nozzle, these minimum velocities could be attained with the blower and control system. A wide range of velocities were covered in these experiments, so that with the different nozzle sizes, a range of turbulent scale structures would be examined.

For each of the first three sets of experiments, the first run was made with the probes nominally set just in the laminar core of the jet. The next two runs were at locations in the initial mixing region. A series of two locations were then examined in the downstream fully developed turbulent mixing region at three different jet velocities. The line array was positioned in the downstream mixing region of the 4 inch diameter nozzle on the flow axis. The jet was operated at two speeds, and all the probes were set to give the v transverse velocity components and then all to give the w velocity components at each jet velocity. The array location point in Table I refers to the center point of the array.

At the present time only a small portion of the raw data acquired has been examined and analyzed in detail. This is because problems have been experienced in writing the required programs for analysis and presentation. Certain preliminary results are given in Chapter 7, and the analysis will be extended to include all the data acquired at a later date.

TABLE I

EXPERIMENTAL RUNS AND CONFIGURATIONS

Run No.	Nozzle Size (in. Diameter)	Nominal Jet Exit Velocity (fps.)	Probe Locations x (in.)	y (in.)	z (in.)	Probe Array And Dimensions
1.1	4	29	12.75	0	0	Square, 0.30 in. spacing between probes
1.2			12.75	1.18		
1.3			12.75	2.36		
1.4			26.5	0		
1.5		29		2.59		
1.6		71		0		
1.7		71		2.59		
1.8		85		0		
1.9	4	85	26.5	2.59	0	
2.1	2.5	111	11.25	0	0	Square, 0.30 in. spacing between probes
2.2			11.25	0.88		
2.3			11.25	1.77		
2.4			17.5	0		
2.5		111		1.22		
2.6		158		0		
2.7		158		1.22		
2.8		171		0		
2.9	2.5	171	17.5	1.22	0	

TABLE I (Cont'd.)

EXPERIMENTAL RUNS AND CONFIGURATIONS

Run No.	Nozzle Size (in. Diameter)	Nominal Jet Exit Velocity (fps.)	Probe Locations x (in.)	y (in.)	z (in.)	Probe Array And Dimensions
3.1	1	56	4.5	0	0	Square, 0.28 in. spacing between probes
3.2			4.5	0.47		
3.3			4.5	0.95		
3.4			7	0		
3.5		56		0.6		
3.6		113		0		
3.7		113		0.6		
3.8		130		0		
3.9	1	130	7	0.6	0	
4.1	4	54	27	0	0	Line 0.30 in. spacing u and v
4.2		42				u and w
4.3		54				u and v
4.4	4	42	27	0	0	u and w

7.0 PRELIMINARY RESULTS

Certain preliminary results will be presented in this chapter. Because the detail programming is not complete, and only a part of the raw data has been treated, no analysis will be attempted. However, some of the results obtained so far will be presented, and the experimental difficulties mentioned. The problem of keeping eight hot-film elements in good working order and fully calibrated will be apparent to anyone who has worked with hot-film anemometers. As the program progressed, techniques for handling the probes and general operating procedures were developed and more consistent results were obtained. However, in several of the first runs, one channel would fail, and the results were incomplete.

The first problem encountered concerned the vibration of the probe supports. This is illustrated by the plots of Figures 15, 16, and 17, which indicate the extent to which this difficulty was overcome. Figure 15 is a plot of the spectrum for the voltage signal recorded by the computer for one channel of a cross-wire probe in the early runs. This result shows that considerable extraneous signals were introduced by vibration of the probe. The spectrum is extremely ragged, and unlike the expected turbulence spectrum. The voltage is a combination of the response to the two velocity fluctuation components, to which the probe is sensitive, and shows considerable high frequency noise. The probe assembly was stiffened and the output signal again recorded. The spectrum formed, this time, is shown in Figure 16. Here a much more representative spectrum was obtained. This result can be criticized as having too high a noise floor, observed as the horizontal line on the plot at the higher frequencies. A final damping and stiffening of the probe and traverse mechanism assembly was made, and the electronics and wire connections improved. The spectrum measured, as shown in Figure 17, provided much better results. The low frequency peak of the previous spectra is eliminated, and a much smoother function formed. The result is typical of the expected turbulent velocity fluctuations in the mixing region of a jet.

This approach was then discontinued since it was not intended to follow the classical statistical analysis of turbulence, but to consider the instantaneous values measured. The voltages measured by the eight channels for a typical run are shown in Figures 18 and 19, where the instantaneous fluctuating component of voltage is plotted against time.

These results were for Run 1.2, where the probe was just in the mixing region of the jet. Channels 1a and 1b are the voltage signals from Probe 1, and are a measure of the voltage due to the $(u + w)$ and $(u - w)$ velocity fluctuations, respectively. Similarly, channels 2a and 2b are also measures of u and w, while channels 3 and 4 are for the u and v velocity components. A total of 200 points are represented, and the time scale is indicated. The voltage scales are normalized on the largest value recorded during the total sample, of which only a part is shown, for convenience.

These results must then be operated on, according to the individual sensitivities of the 8 sensors, and the results converted into the required u, v, and w velocity components. This process is outlined in the chapter on the programs, and utilizes the equations of chapter 4. The results are also calculated in spherical polar velocity coordinates as ρ, θ, and ϕ . Here ρ is the magnitude of the total fluctuating velocity vector, and θ is the angle in the x-y plane measured from the x-axis, and ϕ is the angle the vector makes to this plane. Figure 20 shows some typical results of the program written to calculate these six values. These results are presented for time intervals of 0.0004 second . Examination of the answers produced to date suggests that the correct results are not yet being fully realized. The program is complicated, involving calculation of the wire calibration, and a determination of the separate components for the thousands of data points recorded. The results shown are for the voltages plotted in Figures 18 and 19. The value of the fluctuating velocity component u given in Figure 20 is the mean of the three values calculated for the three probes. The value of the w velocity component is likewise the mean of the two values calculated. The value of v is only that calculated from Probe 3. The results of channel 4a were suspect. Some problems were encountered during acquisition of the data, and the noise was considerably greater on this channel. This technique is only an initial approach to the data analysis.

Examinations of the calculated values show much larger values for the u fluctuating velocity components, and this result dominates the angles calculated for θ. The problem could be due to the probe being too near the laminar core, resulting in very small v and w velocity components, and distorted values for the velocity components in the mean jet flow direction. Unfortunately, at this date, the remainder of the raw data has not been "split", and was therefore unavailable for analysis. This additional data will be examined later during the following program.

A program to visually present the data was also prepared, and it appears to be operating correctly. The results obtained with the data of Run 1.2 will therefore be presented, although again it must be cautioned that the results be considered as preliminary. At present, the program plots every fifth set of values of the data as an isometric drawing of the velocity vector, and the results are shown in Figure 21. In this figure, the x-axis is horizontally to the right, and the y-axis is vertical. The z-axis is then drawn isometrically out of the paper. The velocity vector calculated is transferred to the equivalent isometric values and plotted. Each vector value is plotted with the origin shifted to the right along the x-axis, and so a time scale picture is presented by viewing the drawing to the right. The line drawn is for the equivalent velocity vector when viewed in this isometric presentation. Therefore, the absolute value is not the length of the line, but the sum of the components. However, these are not indicated on the plot, nor is the quadrant within which each vector exists. It was hoped that the result would provide a "picture" of the turbulence. With the limited results and the plot of Figure 21, no immediate

representation is apparent. The lines all tend to lie in one particular direction, making an angle of near +135 to -45 degrees with the x-axis, suggesting that the results of the programs for the velocity components are in question. This conclusion is reached because the data for the voltage plots appears to be perfectly random and valid for turbulence, but the magnitude of the velocity vectors shows such large differences between the longitudinal and transverse velocity components.

Work on these programs is continuing, and the remainder of the data will be examined in due course. The results processed so far must be considered as preliminary, and therefore no analysis of the turbulence structure was attempted.

8.0 CONCLUDING REMARKS

This report presents in detail, the progress at the conclusion of the first phase of the experimental program. The basic apparatus and the multi - hot-wire system have been constructed. The data acquisition system has been setup and some data obtained, for a series of jet flows and nozzle sizes. A range of jet velocities and probe locations have been considered.

Some difficulties have been experienced in developing the programs for the analysis, and the validity of the results obtained to date cannot be confirmed. Some preliminary results have been presented, however, to indicate the scope of the work accomplished so far. This project will be continued during the following program.

In conclusion, the studies have indicated that the technique should be most powerful in studying the basic mechanism of turbulence. A possible method of studying the basic vorticity of the turbulence of a shear flow has been determined, and is presented in the appendices.

REFERENCES

1. Lighthill, M. J., "Sound Generated Aerodynamically, 1 - General Theory", Proc. Roy. Soc. A., 211, (1952).

2. Laurence, J. C., "Intensity, Scale, and Spectra in the Mixing Region of Free Subsonic Jet", NACA Rep. 1292, (1956).

3. Laurence, J. C., "Turbulence Studies of a Rectangular Slotted Noise Suppressor Nozzle", NASA TN D-294, (1960).

4. Davies, P.O.A.L., Fisher, M. J., and Barratt, M. J., "The Characteristics of the Turbulence in the Mixing Region of a Round Jet", Journal Fluid Mech., Volume 15, p. 3, (1963).

5. Davies, P.O.A.L., and Fisher, M. J., "Statistical Properties of the Turbulent Velocity Fluctuations in the Mixing Region of a Round Subsonic Jet", University of Southampton, AASU Rep. 233, (1963).

6. Strasberg, M., "Measurements of the Fluctuating Static and Total Head Pressures in a Turbulent Wake", David Taylor Model Basin, Rep. 1779, (1963).

7. Potter, R. C., "Preliminary Measurements of Pressure Fluctuations in a Shear Layer with Zero Mean Velocity", Wyle Laboratories Research Staff, Report WR 65-15, (1965).

8. Potter, R. C., "Measurement of Pressure Fluctuations in a Turbulent Shear Flow", Paper 3D12 at 72nd Meeting of the Acoustical Society of America, Los Angeles, November (1966).

9. Prandtl, L., 2 angew. Math. u. Mech., Volume 5, (1925), see Goldstein, S., "Modern Developments in Fluid Dynamics", Volume 1, p. 205, Oxford University Press, New York, (1938).

10. Squire, H. B. and Trouncer, J., "Round Jets in a General Stream", British ARC, R and M, No. 1974, (1944).

11. Eldred, K. McK., White, R., Mann, M., and Cottis, M., "Suppression of Jet Noise, with Emphasis on the Near Field", WPAFB, ASD-TDR-62-578, (1963).

12. Taylor, G. I., "Statistical Theory of Turbulence, Parts I-IV", Proc. Roy. Soc. A., Volume 151, (1938).

13. Batchelor, G. K., "The Theory of Homogeneous Turbulence", C.U.P., (1953).

14. Townsend, A. A., "The Structure of Turbulent Shear Flow", C.U.P., (1956).

15. "Handbook of Chemistry and Physics", Thirty-Sixth Edition, Ed. Hodgeman, C. D., Chemical Rubber Pub. Co., Cleveland Ohio, (1954).

16. Minzner, R. A., Champion, K.S.W., and Pond, H. L., "The ARDC Model Atmosphere, 1959", AF CRC-TR-59-267.

17. Hilsenrath, J., et al, "Tables of Thermodynamic and Transport Properties of Air, Argon, Carbon Dioxide, Carbon Monoxide, Hydrogen, Nitrogen, Oxygen, and Steam", Pergamon Press, New York, (1960).

18. Potter, R. C., "The Hot Wire Anemometer", Wyle Laboratories Research Staff Report WR 64-8, (1964).

APPENDIX A

EXPERIMENTAL PROCEDURE

The acquisition and storage of data by the computer is the final step in a series of preparatory steps which take a week to four days for completion by present methods. The important steps leading to acquisition of eight channels of voltage fluctuations which can be interpreted in terms of turbulent velocity fluctuation are itemized below.

1. The traversing gear and probe mounts are aligned and leveled to correspond with the geometrical nozzle axis.

2. The jet is traversed by a pitot static tube-thermocouple arrangement vertically and horizontally at two or more axial distances downstream. Using this data the velocity profiles can be calculated using the program, "POS", in Appendix B.

3. The center of the velocity profiles is used to determine the traverse mechanism settings which define the axis of the jet.

4. The probes are mounted and the traverse mechanism settings determined for the measurements to be made.

5. Constants important to the calibration and computer acquisition of the data are now recorded. These include the atmospheric pressure, the humidity, the voltage at zero velocity for each of the eight channels, the probe spacings, and the relative probe positions.

6. Calibration is carried out with the hot film probes and a pitot static tube-thermocouple arrangement in the potential core of the jet. The jet velocity is varied by the valving arrangement on the blower. These valve settings are predetermined to give about ten well spaced points over the velocity range of interest.

7. Several sets of data are sent to the computer for a single calibration according to the predetermined experimental program. For each set of data the values of the mean voltage, E_m, are determined for each channel, so that the sensitivity, S, can be determined from the calibration. After each set of data has been acquired by the computer, the traversing gear and/or valving system is brought to the new predetermined settings and new valves of E_m recorded for each channel

prior to the next computer aquisition.

8. Atmospheric pressure, the voltage at zero velocity, and the humidity are again noted after the random data has been acquired and stored by the computer.

APPENDIX B

COMPUTER PROGRAMS

Five programs have been developed to facilitate data reduction during the study of the macroscale of turbulence. These will be discussed briefly in order of their occurrence on the following pages. This order corresponds roughly to the order in which they have been and will be applied to data reduction and processing. One of the programs, entitled "CALIB", is not presented because of difficulty in incorporating a useful subroutine for a least square first order polynomial fit of calibration data into the general scheme of calibration data analysis. Since the program is currently being run in two parts and will shortly be modified, it will be presented at a later date.

Program "POS" is used to determine the horizontal and vertical velocity profiles of the jet axis. This axis is then the reference from which horizontal distances are measured. The form of the program presented here included the temperature and humidity correlations discussed in Section 3.

Subroutine "PLOTIT" is used to plot out the random voltage signals acquired on the eight channels for visual inspection. This makes it possible to determine whether the data has been properly acquired stored and ordered on the digital tape.

Program "MILPOT" uses inputs from program "CALIB", Em values determined during a data acquisition, and random voltage signals on the eight anemometer channels, to determine and print the values of u and v or u and w from each set of crossed hot film sensors. An ensemble average of u, v, and w over the four sets of sensors is also produced and printed out.

Program "TRIPLOT" is used to provide an isometric plot of values of u, v, and w which are inputs from program "MILPOT". This program will undergo changes shortly which should make it possible to identify the quadrant in which the fluctuating velocity vector is plotted.

Since most of these programs have recently been developed improvements and modifications are to be expected. Any such changes shall be reported in subsequent reports.

```
      PROGRAM POS
      DIMENSION ICARD(20)
4     READ(60,6)ICARD
6     FORMAT(20A4)
      READ(60,7)I
7     FORMAT(I3)
      WRITE(61,8)ICARD
8     FORMAT(1H1,20A4/)
      WRITE(61,5)
5     FORMAT(9X4HT(0),12X4HP(0),13X1HP,11X4HP(A),13X1HU,/)
      READ(60,2)PA1,HR
2     FORMAT(8F10.0)
      DO 9 N=1,I
      READ(60,2)T,PO,P,RHO,RHO1,TR
1     FORMAT(5F10.0)
      T=T+459.688
      PA=(RHO/RHO1)*PA1
      R=49720.
      PSAT= 1.714E-05 *TR*TR-(1.735E-02*TR) + 4.4068
      XX=29.92*HR*(PSAT/PA)
      GAM=1./(.4*(1.-XX)*(XX/.3))
      GAM=GAM+1.
      FM=28.966*(1.-XX)+34.012*XX
      P=P/2.
      X1=2.*GAM/(GAM-1.)
      X2=R*T/FM
      X3=(P+PA)/(PO+PA)
      X4=(GAM-1.)/GAM
      X5=X3**X4
      X6=1.-X5
      XU=SQRTF(X1*X2*X6)
9     WRITE(61,3)T,PO,P,PA,XU
3     FORMAT(5(5XF10.4)/)
      GO TO 4
      END
```

Program 1 - "POS"

```
      SUBROUTINE PLOTIT(A,KMAX)
      DIMENSION A(256)
      YX=4.
      XMIN=XMAX=0.
      DO 50 K=1,KMAX
      IF (XMAX.GT.A(K)) 45,40
   40 XMAX=A(K)
   45 IF (XMIN.LT.A(K)) 50,48
   48 XMIN=A(K)
   50 CONTINUE
      WRITE (61,501) XMAX,XMIN
      AX=ABSF(XMAX)
      AY=ABSF(XMIN)
      IF (AX.GT.AY) 53,51
   51 XSTR=AY
      GO TO 54
   53 XSTR=AX
   54 SCALE=1.
   55 XMAX=XSTR*SCALE
      IF (XMAX.LT.1.) 60,70
   60 SCALE=SCALE*2.
      GO TO 55
   65 XMAX=XSTR*SCALE
   70 IF (XMAX.GT.YX) 75,80
   75 SCALE=SCALE/2.
      GO TO 65
   80 WRITE (61,500) SCALE
      DELTAX=8./FLOATF(KMAX)
      CALL PLOTCON
      Y=0.
      DO 100 K=1,KMAX
      X=A(K)*SCALE
      CALL PLOT (X,Y,2)
  100 Y=Y+DELTAX
      CALL PLOT (0.,Y,3)
      CALL PRINTCON
      RETURN
      ENTRY START
      WRITE (59,525)
      PAUSE
      CALL PLOTCON
      CALL PLOT (0.,0.,-3)
      CALL PLOT (-4.,0.,2)
      CALL REALAXIS (4.,64.,4.,8.,0)
      CALL PLOT (0.,0.,3)
      CALL PRINTCON
      RETURN
  500 FORMAT (10X,13HSCALE FACTOR=,E16.8)
  501 FORMAT (10X,5HXMAX=,E16.8,5X,5HXMIN=,E16.8)
  525 FORMAT (2X,50HPOSITION PLOTTER PEN IN CENTER OF PAGE AND PUSH GO)
      END
```

Program 2 - "PLOTIT"

```
      PROGRAM MILPOT
      COMMON UU,VV,WW,F
      DIMENSION EO(4,2),EM(4,2),H(4,2),Z(4,2),U(200,4),V(200,4),
     CUU(200),VV(200),WW(200),RO(200),THTA(200),PHI(200),E(200,4,2)
      DIMENSION XXX(200),LABEL(4),IX(1000),ID(2)     ,S(4,2)
      EQUIVALENCE(E(1),U(1))
      EQUIVALENCE(XXX(1   ),VV(1))
      EQUIVALENCE(E(801),V(1))
      PAUSE 5
      READ(60,22)(( H(I,J),J=1,2),I=1,4)
      READ(60,22)(( Z(I,J),J=1,2),I=1,4)
      READ(60,22)((EO(I,J),J=1,2),I=1,4)
      READ(60,22)((EM(I,J),J=1,2),I=1,4)
      READ(60,21)DA,TE,                                    THETA
      PAUSE 1
99     FORMAT(5E15.5)
21    FORMAT(13E6.0)
22    FORMAT( 8E6.0)
      DO 1 I=1,4
      DO 1 J=1,2
      S(I,J)=H(I,J)*Z(I,J)**(1./H(I,J))*((EM(I,J)**2-EO(I,J)**2)**(1.-1.
     C/H(I,J)))/(2.*EM(I,J))
1     CONTINUE
      MAX=1000
      CALL START (DUM,DUM)
      CALL PRINTCON
      DO 200 J=1,2
      DO 200 I=1,4
      CALL READCON
   24 READ (60,500) ID(1),ID(2)
      CALL TAPE (3,1,LABEL(1),LABEL(2),II)
      GO TO (25,300,320) II
   25 CALL TAPE (3,1,IX(1),IX(MAX),II)
      GO TO (30,40,320) II
   30 IF (LABEL(1).EQ.ID(1)) 35,25
   35 IF (LABEL(2).EQ.ID(2)) 50,25
   40 CALL TAPE (3,1,LABEL(1),LABEL(2),II)
      GO TO (25,300,320) II
   50 CALL PRINTCON
      WRITE (61,501)ID(1),ID(2)
      N=0
      DO 60 K=1,MAX,5
      N=N+1
   60 E(N,I,J)=XXX(N)=FLOATF(IX(K))          *.001
      CALL PLOTIT (XXX, N )
      CALL PLOTCON
      CALL PLOT(4.,8.,-3)
      CALL PRINTCON
  200 CONTINUE
      GO TO 350
  300 WRITE (61,502)
      PAUSE $ GO TO 24
  320 WRITE (61,503)
      PAUSE  $  GO TO 24
```

Program 3 - "MILPOT"

```
 350 CONTINUE
 500 FORMAT (A4,A4)
 501 FORMAT (10X,2A4,2X,25HIS THE CHANNEL BEING USED)
 502 FORMAT (10X,13HBAD TAPE READ)
 503 FORMAT (10X,12HPARITY ERROR)
     DO 10 I=1,4
     DO 10  K=1,200
     V(K,I)=(E(K,I,1)/S(I,1)-E(K,I,2)/S(I,2))/2./COS (THETA)
     U(K,I)=(E(K,I,1)/S(I,1)+E(K,I,2)/S(I,2))/2./SIN (THETA)
10   CONTINUE
     WRITE(61,99)    U
     WRITE(61,99)    V
     DO 11  K=1,200
     VV(K)=(         V(K,2))/1.
     UU(K)=(         U(K,2)+U(K,3)+U(K,4))/3.
     WW(K)=(V(K,3)+V(K,4))/2.
     RO(K)=SQRT (UU(K)**2+VV(K)**2+WW(K)**2)
     THTA(K)=ATAN (VV(K)/UU(K))
     PHI(K)=ATAN (WW(K)/SQRT (UU(K)**2+VV(K)**2))
11   CONTINUE
     WRITE(61,1000)
     WRITE(61,1001) (UU(K),VV(K),WW(K),RO(K),THTA(K),PHI(K),K=1,200)
     WRITE(59,1002) $ PAUSE
     CALL TRIPLOT
     PAUSE 1
1000 FORMAT(1H1,7X2HUU,16X2HVV,16X2HWW,16X2HRO,15X,4HTHTA,15X3HPHI/)
1001 FORMAT(6E18,8)
1002 FORMAT(5X32HMOVE PEN TO CENTER PAGE, PUSH GO/)
     END
```

Program 3 – "MILPOT" (Continued)

```
      SUBROUTINE TRIPLOT
      COMMON UU,VV,WW
      DIMENSION UU(200),VV(200),WW(200)
      DT=0.0
      SQ=1.0/SQRT(2.0)
      CALL PLOTCON
      CALL PLOT(0.0,4.0,-3)
      CALL REALAXIS(-4.0,0.0,2.0,2.0,0)
      CALL REALAXIS(0.0,50.0,2.0,8.0,0)
      CALL PLOT(2.0,-2.0,2)
      DO 70 K=1,200
      VV(K)=-WW(K)*SQ+VV(K)
   70 UU(K)=-WW(K)*SQ+UU(K)
      XMAX=XMIN=0.
      DO 90 K=1,200
      IF(XMAX.GE.VV(K))82,81
   81 XMAX=VV(K) $ GO TO 90
   82 IF(XMIN.LE.VV(K))90,84
   84 XMIN=VV(K)
   90 CONTINUE
      XM=ABS(XMAX) $ YM=ABS(XMIN)
      IF(XM.GE.YM)100,95
   95 XM=YM
  100 XM=4.0/XM
      YM=XM/10.
      DO 200 K=1,200
      Y=UU(K)*YM+DT
      X=VV(K)*XM
      CALL PLOT(0.0,DT,3)
      CALL PLOT(X,Y,2)
  200 DT=DT+.25
      RETURN
      END
```

Program 4 - "TRIPLOT"

APPENDIX C

CALCULATION OF VORTICITY VECTOR

The probe arrangment of 4 cross wire pairs in a square will allow the vorticity vector for the flow to be calculated. The computer program will output the 4 values of the u velocity fluctuations and the 2 values of the v and w velocity fluctuations at the four corners of the array. With the wires arranged as shown in the sketch below, and the velocity components numbered according to the wires, the vorticity vector can be determined.

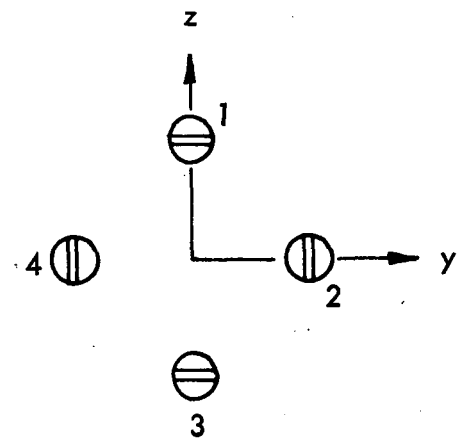

Sketch of wires and probes looking downstream onto the array

For example the velocity component w_2 is the component measured by probe 2, in the direction z.

The vorticity vector $\underset{\sim}{\Gamma}$ is defined by

$$\underset{\sim}{\Gamma} = (\xi, \eta, \zeta)$$

where

$$\xi = \left(\frac{\partial w}{\partial y} - \frac{\partial v}{\partial z}\right)$$

$$\eta = \left(\frac{\partial u}{\partial z} - \frac{\partial w}{\partial x}\right) \qquad \text{(C.1)}$$

$$\zeta = \left(\frac{\partial v}{\partial x} - \frac{\partial u}{\partial y}\right)$$

For the evaluation we will use

$$\xi = \frac{(w_2 - w_4)}{\Delta y} - \frac{(v_1 - v_3)}{\Delta z}$$

$$\eta = \frac{(u_1 - u_3)}{\Delta z} - \frac{1}{2U}\left(\frac{dw_2}{dt} + \frac{dw_4}{dt}\right)$$

$$\zeta = \frac{1}{2U}\left(\frac{dv_1}{dt} + \frac{dv_3}{dt}\right) - \frac{(u_2 - u_4)}{\Delta y} \qquad \text{(C.2)}$$

to give the required vorticity components at each instant of time.

Δy and Δz, the separations of the probes, and U, the mean velocity, will be input constants to the program, and obtained directly from measurements of the probe and the mean velocity calibration.

$\frac{dw}{dt}$ may be evaluated by any desired differentiation technique of the digital data.

The method of Equation (C.2) is based on the assumption of Taylor's Hypothesis to determine the rate of change of the velocity components in the x direction, the direction of the mean flow. Because of the problem of probe interference, it will not be possible to arrange a series of wires downstream of the array to measure the space rate of change of the velocity components. It is assumed that the turbulence is convected unchanged over the short distance of separation in the x axis equal to the probe separation in the other two axes. Because the time for the flow pattern to be swept this distance downstream is very short, the turbulence pattern will only change slightly in the small time inferred. The validity of this approach has been confirmed in several experimental investigations, notably that of Taylor himself (Reference 12), in his study of the relationship between correlation and spectra.

APPENDIX D

THE USE OF PLANAR ARRAYS OF CROSSED HOT FILM SENSORS TO MEASURE THE INSTANTANEOUS TRANSVERSE SCALE OF TURBULENCE IN A JET

This report deals with the use of a planar array of four sets of crossed hot film sensors, to determine fluctuating velocity components. Appendix C discusses how the vorticity vector may be determined experimentally.

A larger planar array of crossed sensors suggests an interesting method of experimentally determining the transverse scale of turbulence in a jet. The transverse scale defines a representative eddy dimension in a plane perpendicular to the mean flow direction of a jet. Such a large planar array of crossed hot film sensors is illustrated in the sketch below. The array is in the plane of the paper and the mean flow direction is perpendicular to the page and directed toward it. The symbol L, describes the distance from the center of a four probe configuration which is chosen as the center of the array to some point in the array. Each line represents a hot film sensor. Each pair of lines (sensors) are skewed at equal but opposite angles, θ, into the page.

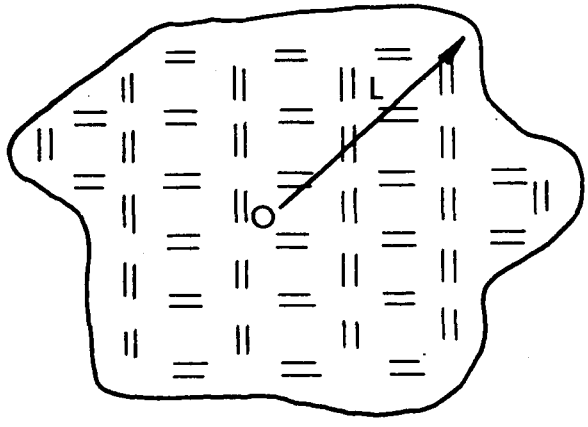

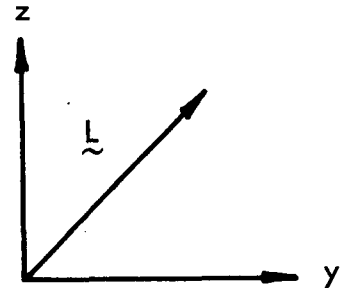

$$\underset{\sim}{L} = z\hat{k} + y\hat{j}$$

$$L = (z^2 + y^2)^{1/2}$$

Sketch of Planar Anemometer Array

The entire area of the array may be broken up into small square elements, each of which is bounded by four probes arranged as shown in sketch below.

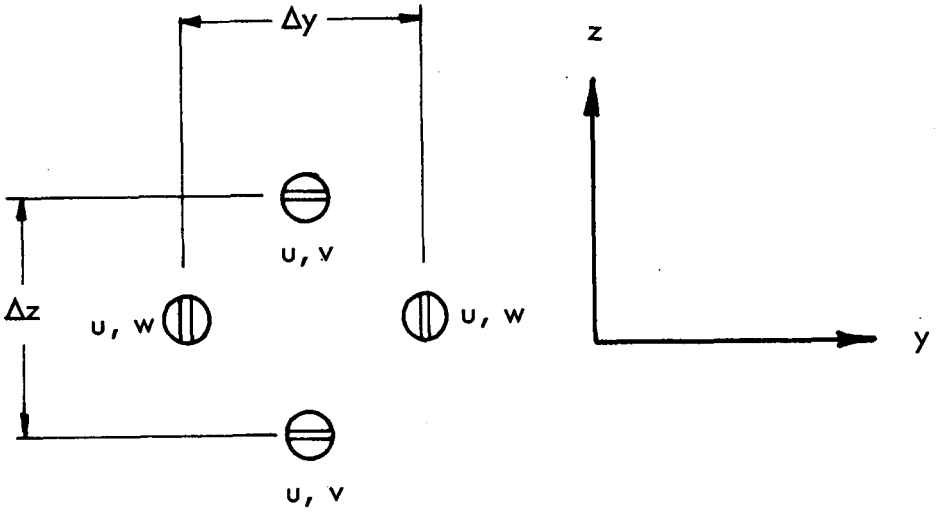

Sketch of 4 Probe Array Showing Dimensions and Velocity Components

The setsof crossed hot film sensors are labeled with the fluctuating velocity components which they measure.

This probe arrangement permits the calculation of the vorticity component perpendicular to the plane of the probes or parallel to the mean flow velocity according to the equation,

$$\xi = \left(\frac{\partial w}{\partial y} - \frac{\partial v}{\partial z}\right) \tag{D1}$$

A useful theorem to consider when dealing with the probe array is Stoke's theorem for a planar surface. In the notation used here it is,

$$\oint v\,dy + \oint w\,dz = \iint \left(\frac{\partial w}{\partial y} - \frac{\partial v}{\partial z}\right) dy\,dz \tag{D2}$$

integrals along a closed path

Since we are dealing with a practical case we may replace $dy\,dz$ by $\Delta y\,\Delta z$, ∂w and ∂v by Δw and Δv, and the double integral sign with a double summation sign as in the following equation,

$$\oint v\,dy + \oint w\,dz = \sum_i \sum_j \left(\frac{\Delta w}{\Delta y} - \frac{\Delta v}{\Delta z}\right)_{ij} \Delta y_i\, \Delta w_j \qquad \text{(D3)}$$

where i, j designate a particular element of the array, Δy_i Δz_j, and measured velocity gradients associated with that area, $\Delta w/\Delta y$ and $\Delta v/\Delta z$. This equation states that product of the area element determined by four probes and the vorticity component, ξ measured by the probes, summed over an extended area is equal to the component of velocity tangent to a boundary element which is integrated around the boundary of the extended area. The area considered is, of course, planar.

Returning now to the first sketch of the probe array, it is not difficult to imagine a method of determining the transverse scale of turbulence.

With all sensors operating, a computer system, similar to that employed in the experimental work discussed in this report records instantaneous voltages for calculation of a set of values of v and w over the array. These data may later be analyzed by assuming, for simplicity, that $4yz$ is the observed arbitrary area. This area is symmetrical about the center as shown in the sketch of the array. Then the expression

$$\frac{1}{4yz} \sum_{i=1}^{n} \sum_{j=1}^{n} \left(\frac{\Delta w}{\Delta y} - \frac{\Delta v}{\Delta z}\right)_{ij} \Delta y_i\, \Delta z_j = \frac{1}{4yz}\left[\oint v\,dy + \oint w\,dz\right] \qquad \text{(D4)}$$

may be evaluated. It is convenient to represent the velocity component tangent to a small arbitrary element of boundary and integrated around the boundary of the area $4yz$ by the symbol C, where

$$C = \frac{1}{4yz}\left[\oint v\,dy + \oint w\,dz\right] \qquad \text{(D5)}$$

Similarly if the computer approximated a circle in observing an area of arbitrary size the average vorticity over the arbitrary area would be

$$C = \frac{1}{\pi(y^2 + z^2)} \sum_{i=1}^{n} \sum_{j=1}^{n} \left(\frac{\Delta w}{\Delta y} - \frac{\Delta v}{\Delta z} \right)_{i\,j} \Delta y_i \, \Delta z_j \qquad \text{(D6)}$$

Thus, the shape of the area analyzed may be variable.

Providing that the transverse turbulent scale is large compared with the smallest area element, $\Delta y \, \Delta z$, a plot of C versus L, or some other representative coordinate such as y or z in the case of Equation (D4), will show a maximum. This will occur when the chosen coordinate gives an area and shape which corresponds to the size of the section of an eddy centered roughly on the origin, O. Also the origin O may be shifted to map vortices over the array. The type of graph to be expected in general for an origin corresponding to the center of an eddy, is shown in the following sketch:

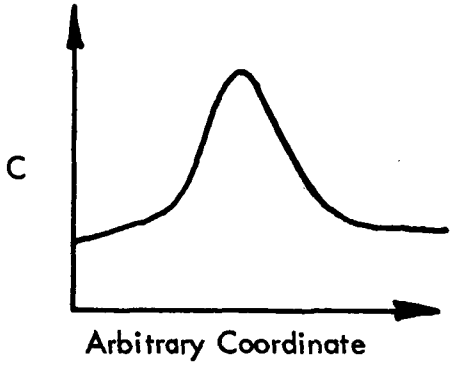

Sketch of C Versus an Arbitrary Coordinate

The value of the arbitrary coordinate, for instance $(y^2 + z^2)^{1/2}$, at the peak of the curve should give a good indication of the instantaneous turbulent scale. It is also interesting that C has the dimensions of frequency. This suggests that the peak height may provide information on the transverse turbulent spectra if a large number of samples are taken over an extended time period and analyzed.

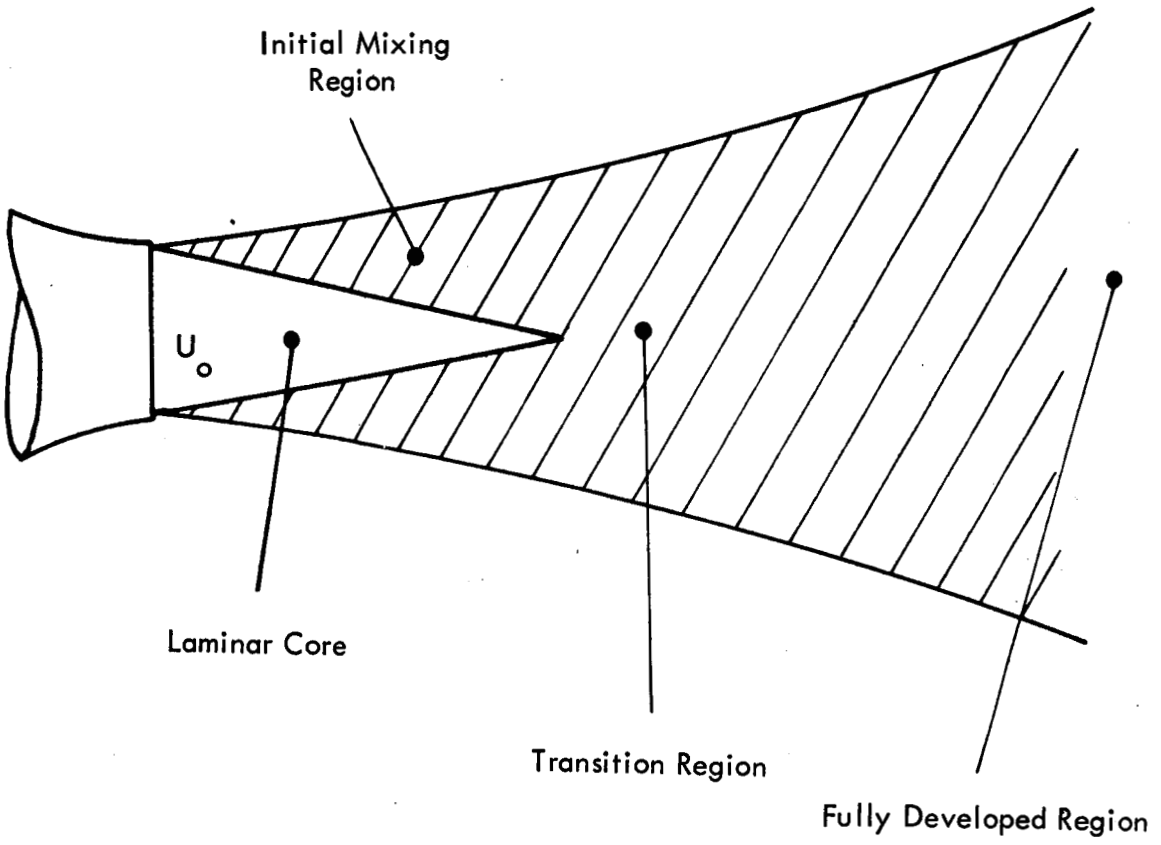

Figure 1. Mixing of a Subsonic Jet

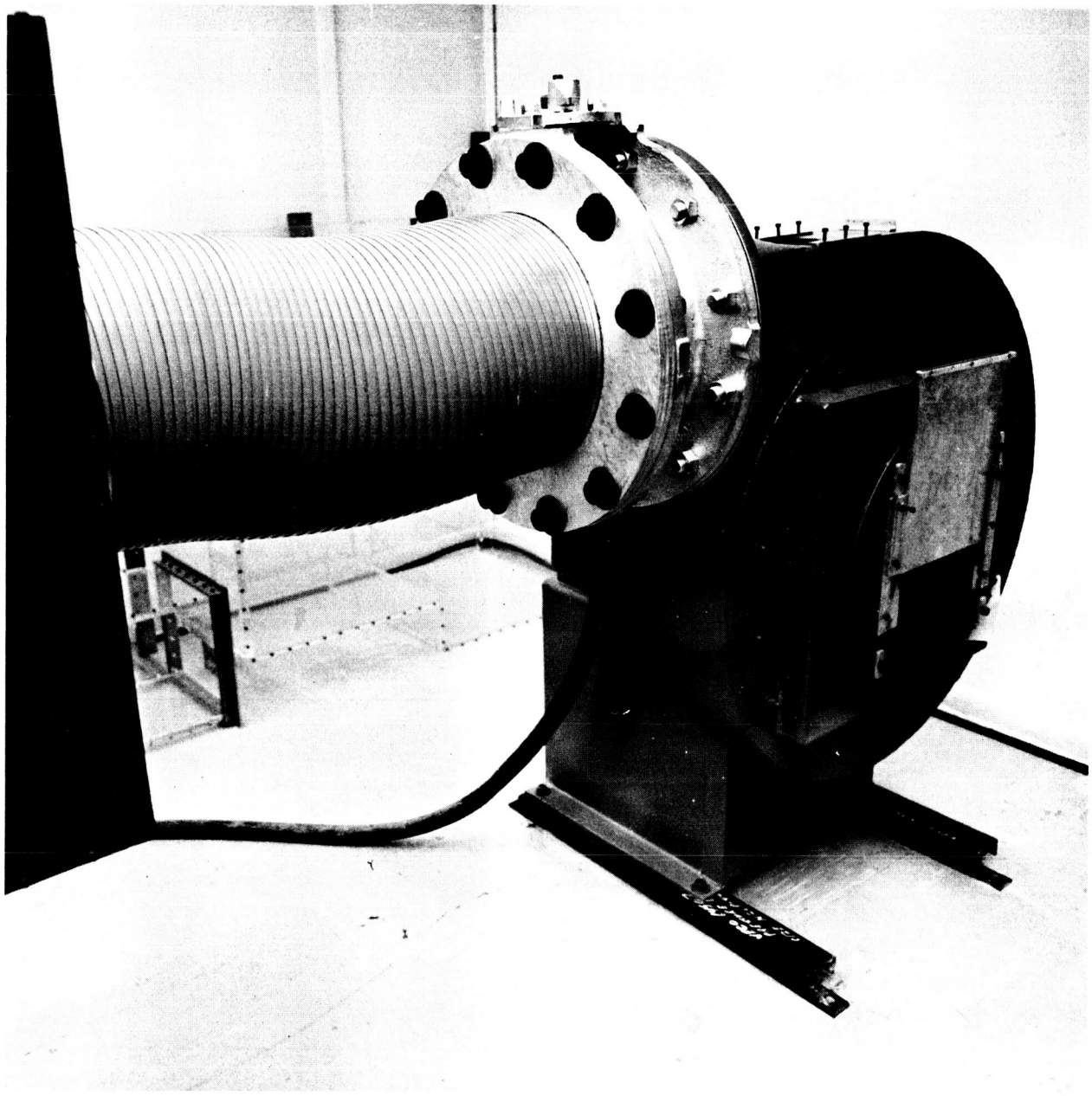

Figure 2: Blower

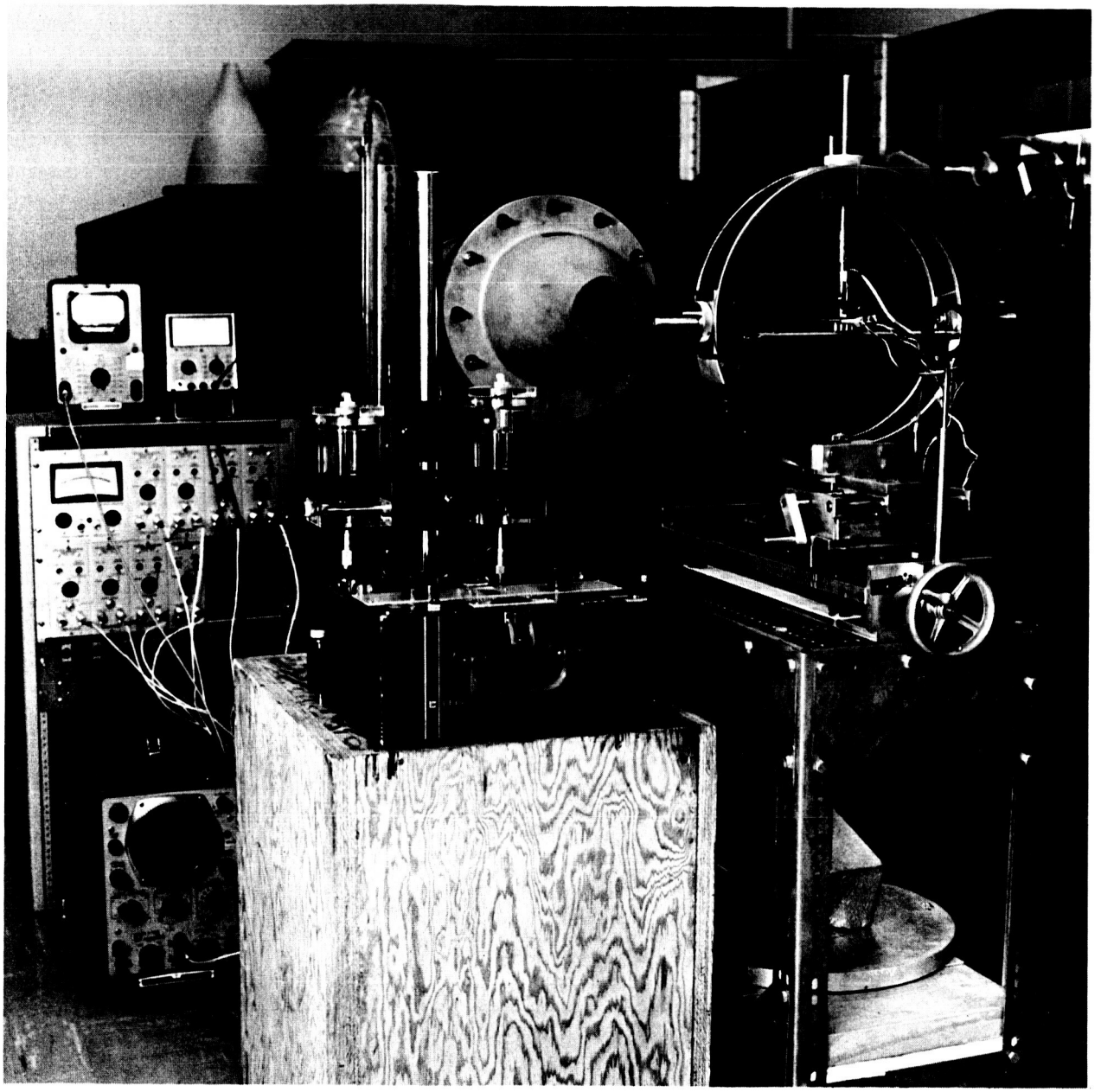

Figure 3: General View of Rig

4" Exit Diameter Nozzle

DIMENSIONS

y inch	x inch rad.
0	5.125
1	5.06
2	4.91
3	4.64
4	4.18
5	3.49
6	2.94
7	2.58
8	2.31
9	2.11
10	2.00

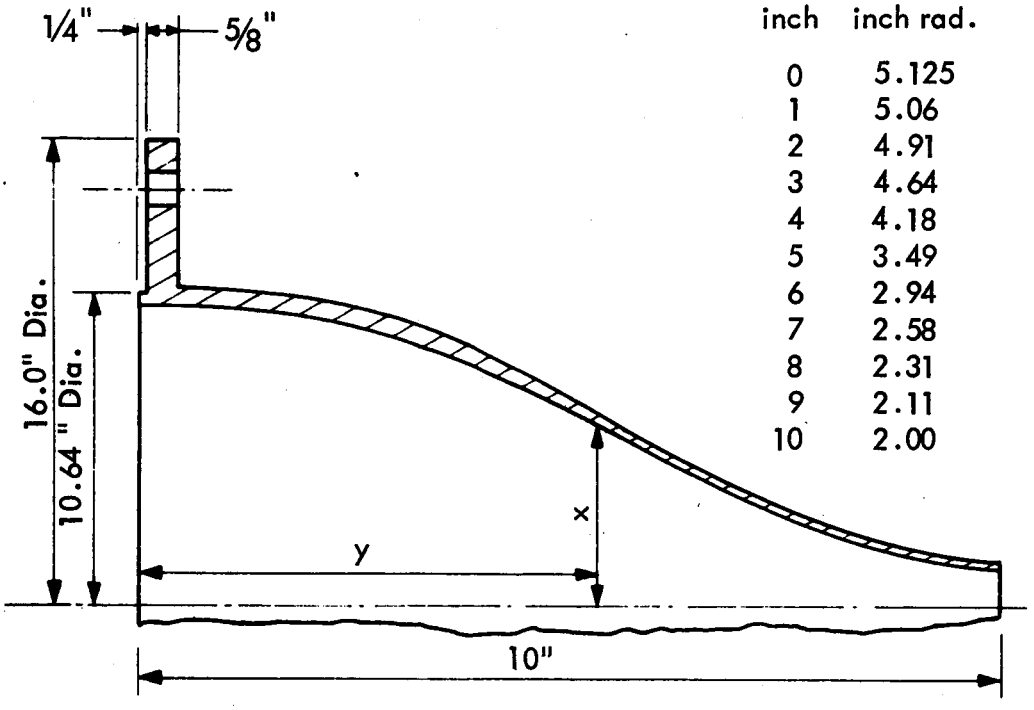

Figure 4a. Dimensions of 4" Exit Diameter Nozzle

1" Exit Diameter Nozzle DIMENSIONS		2.5" Exit Diameter Nozzle DIMENSIONS	
y inch	x inch rad.	y inch	x inch rad.
0	5.125	0	5.125
1	5.10	1	5.125
2	5.01	2	5.094
3	4.85	3	5.015
4	4.64	4	4.875
5	4.33	5	4.656
6	3.97	6	4.344
7	3.60	7	3.906
8	3.09	8	3.438
9	2.56	9	2.969
10	2.06	10	2.500
11	1.60	11	2.015
12	1.10	12	1.625
13	0.815	13	1.344
14	0.645	14	1.250
15	0.500	15	1.250

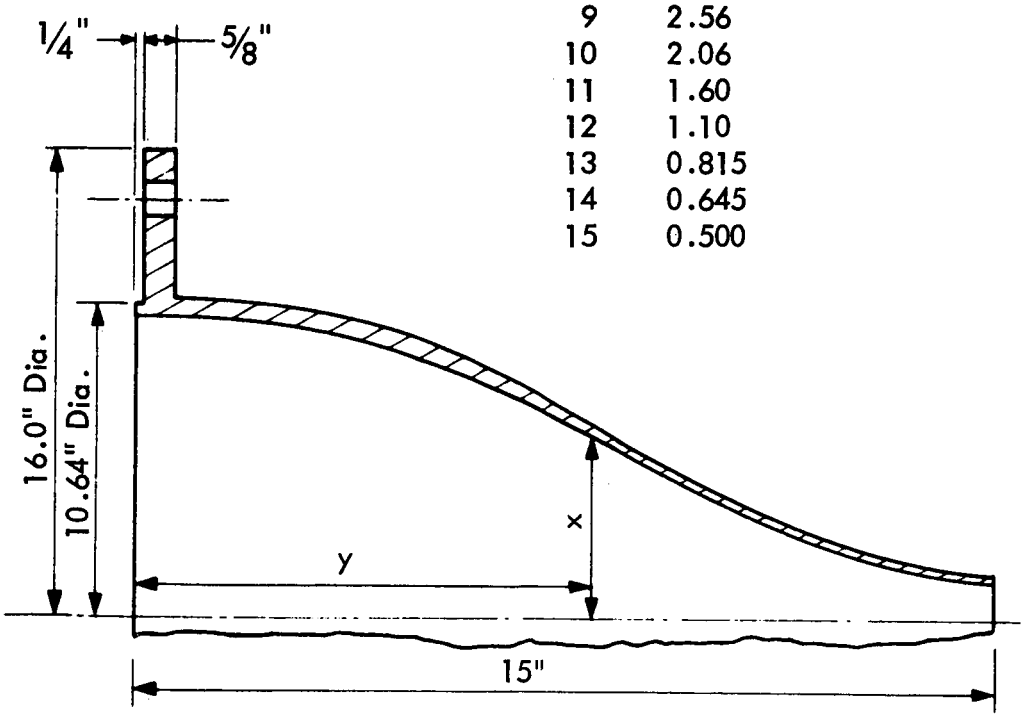

Figure 4b. Dimensions of 1" and 2.5" Exit Diameter Nozzles

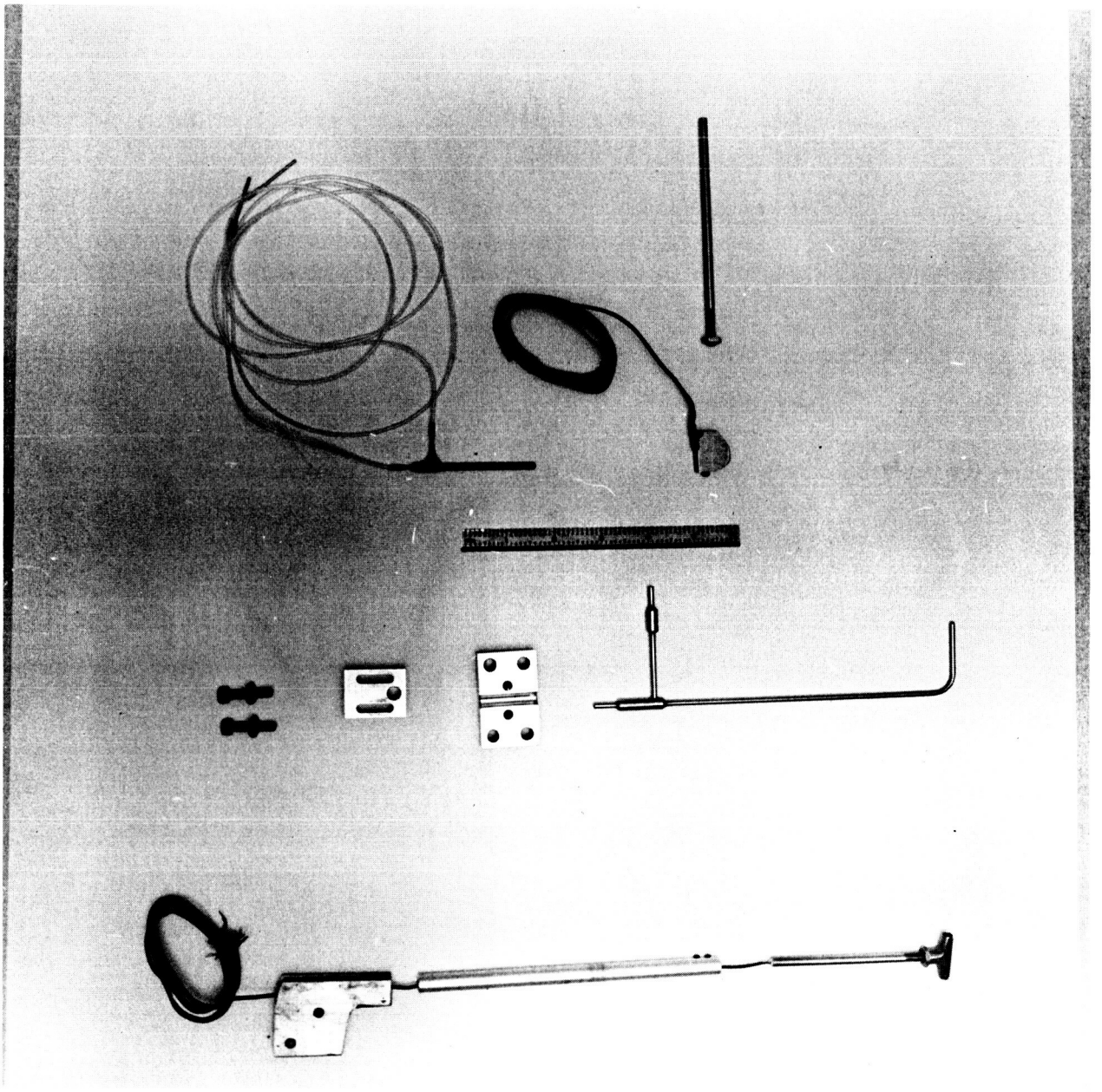

Figure 5: Mean Velocity and Temperature Probes

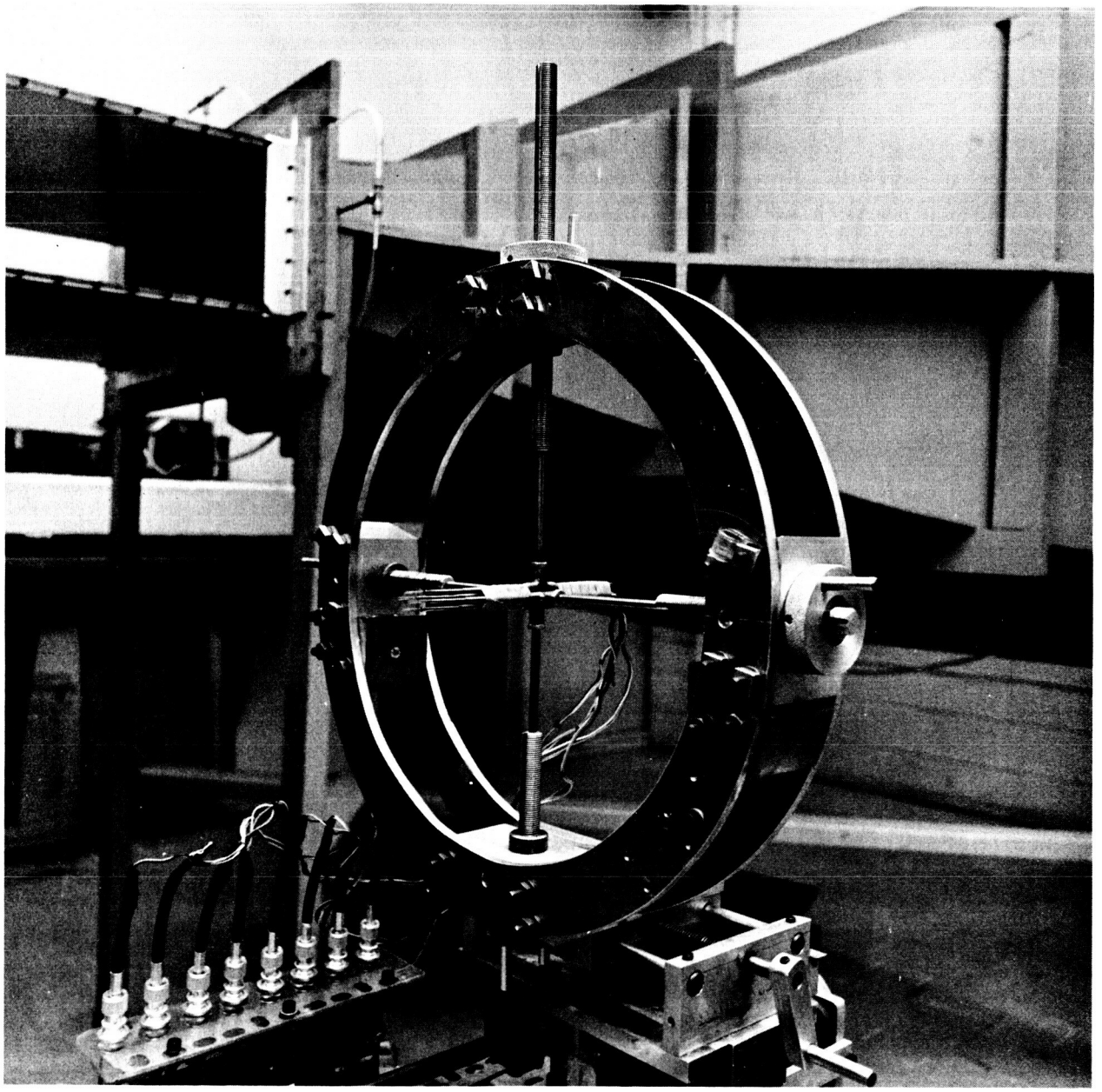

Figure 6: Square Probe Array

Figure 7: Sensor Elements

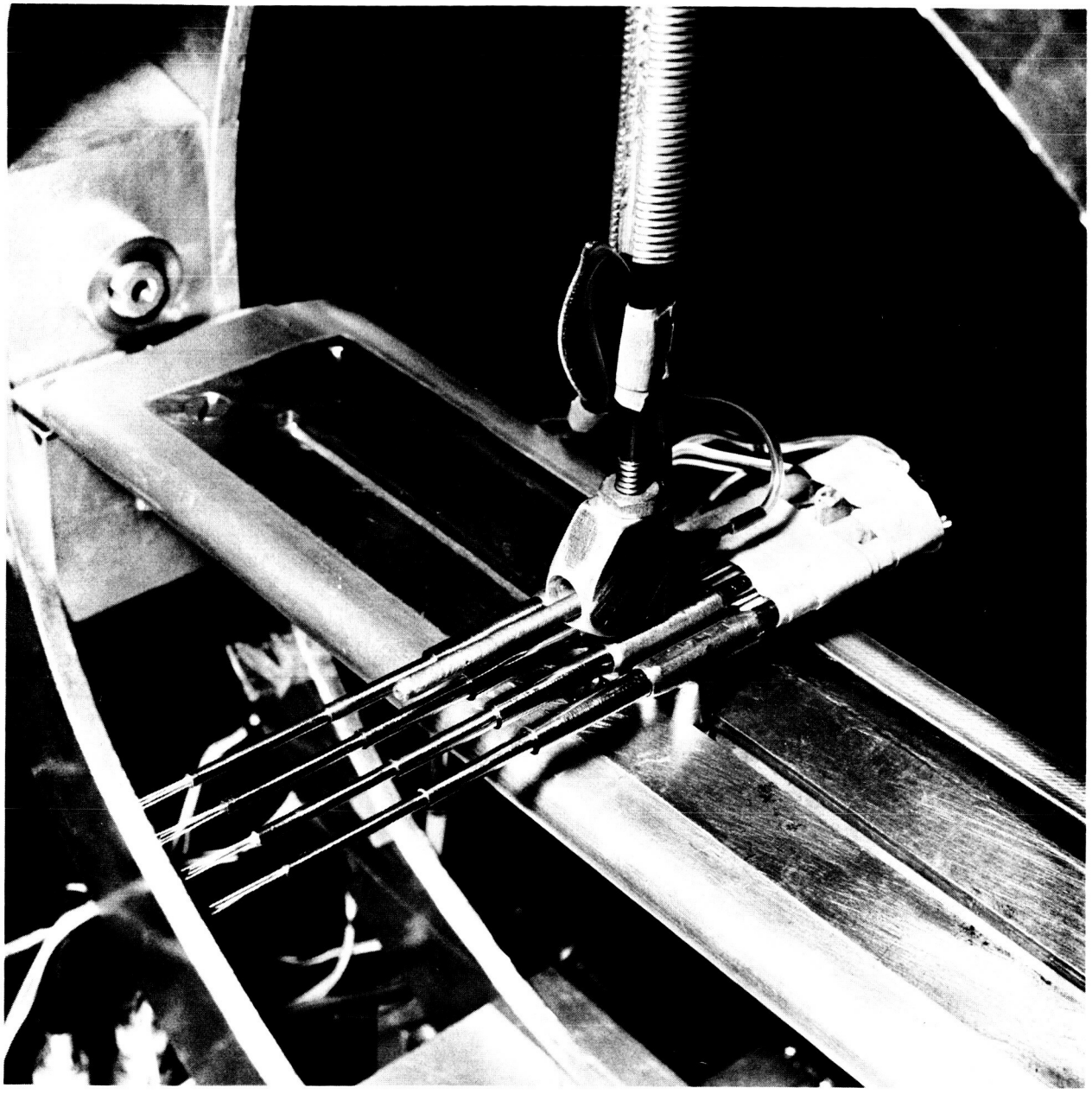

Figure 8: Line Probe Array

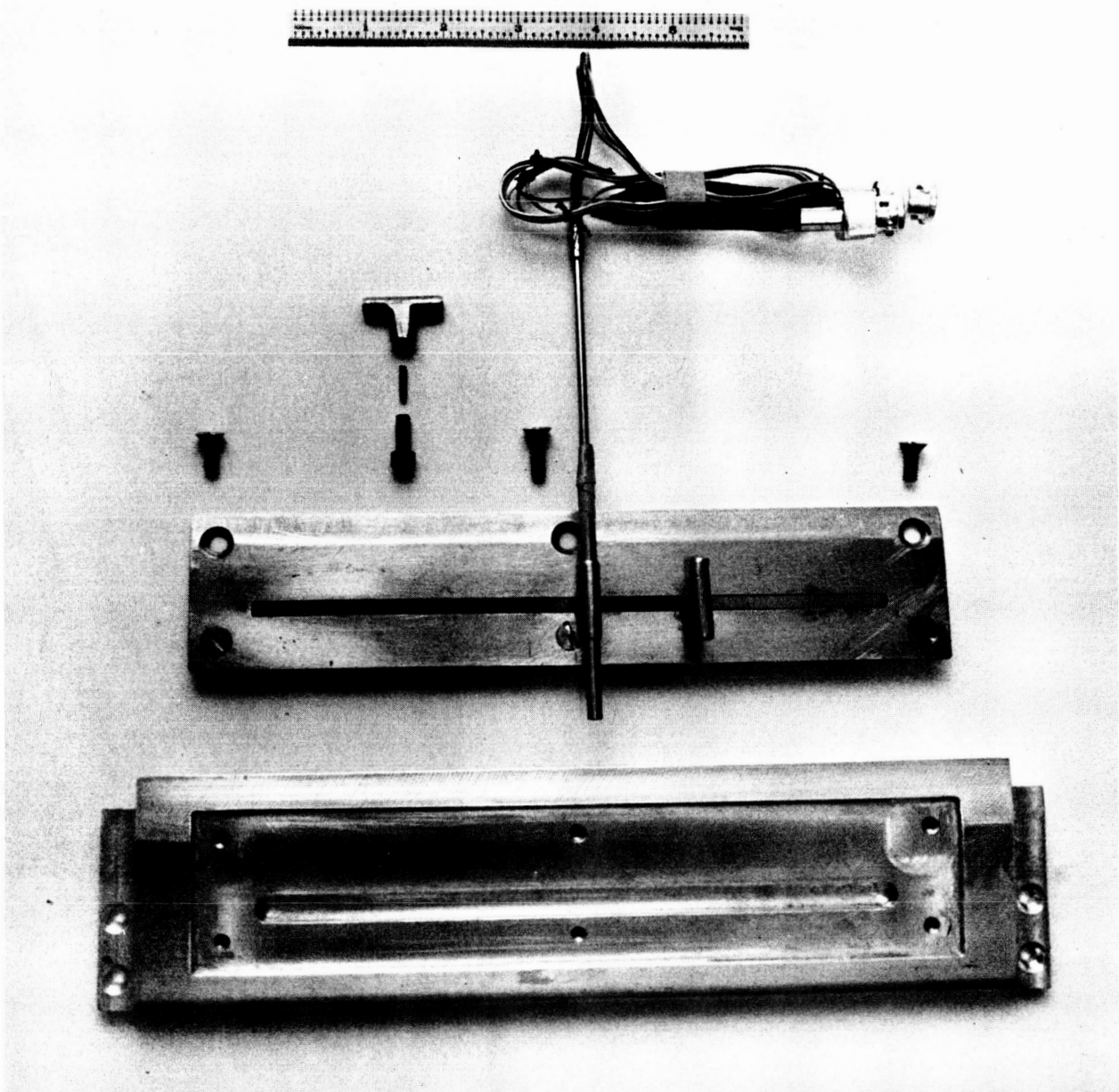

Figure 9: Airfoil for Line Probe Array

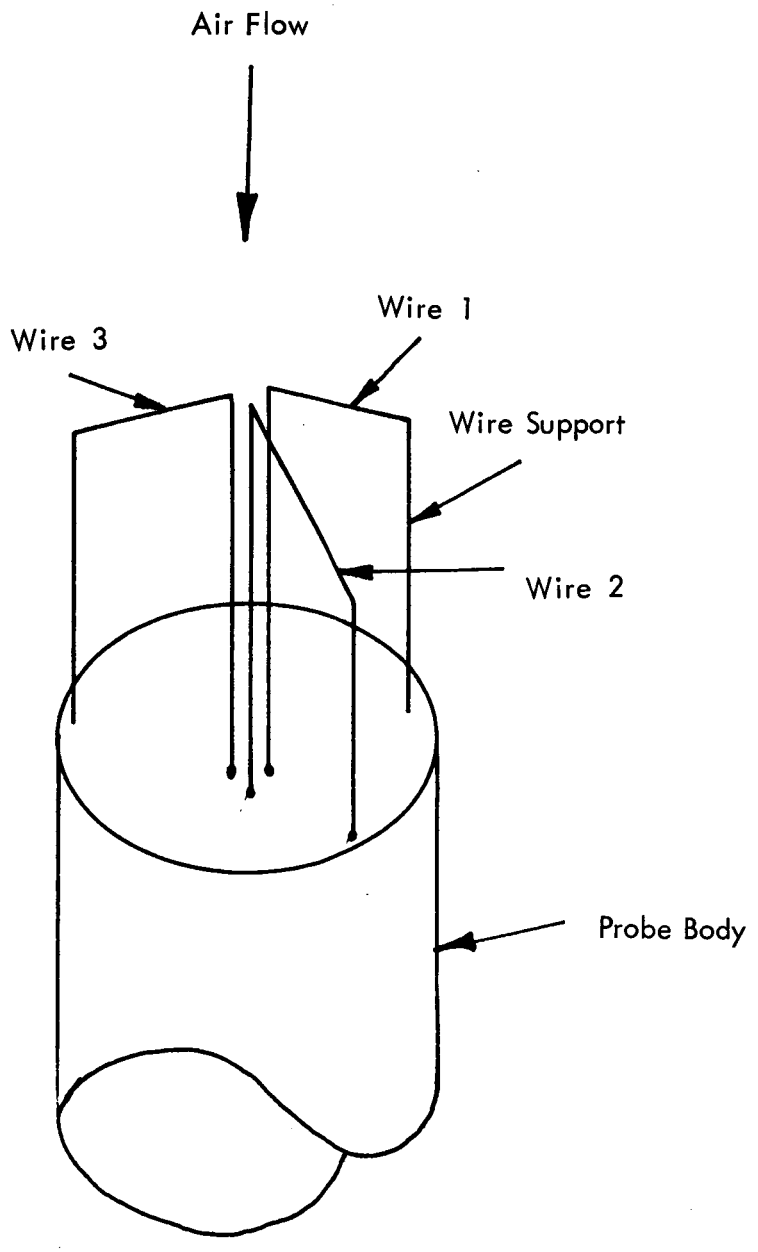

Figure 10. Three Wire Probe

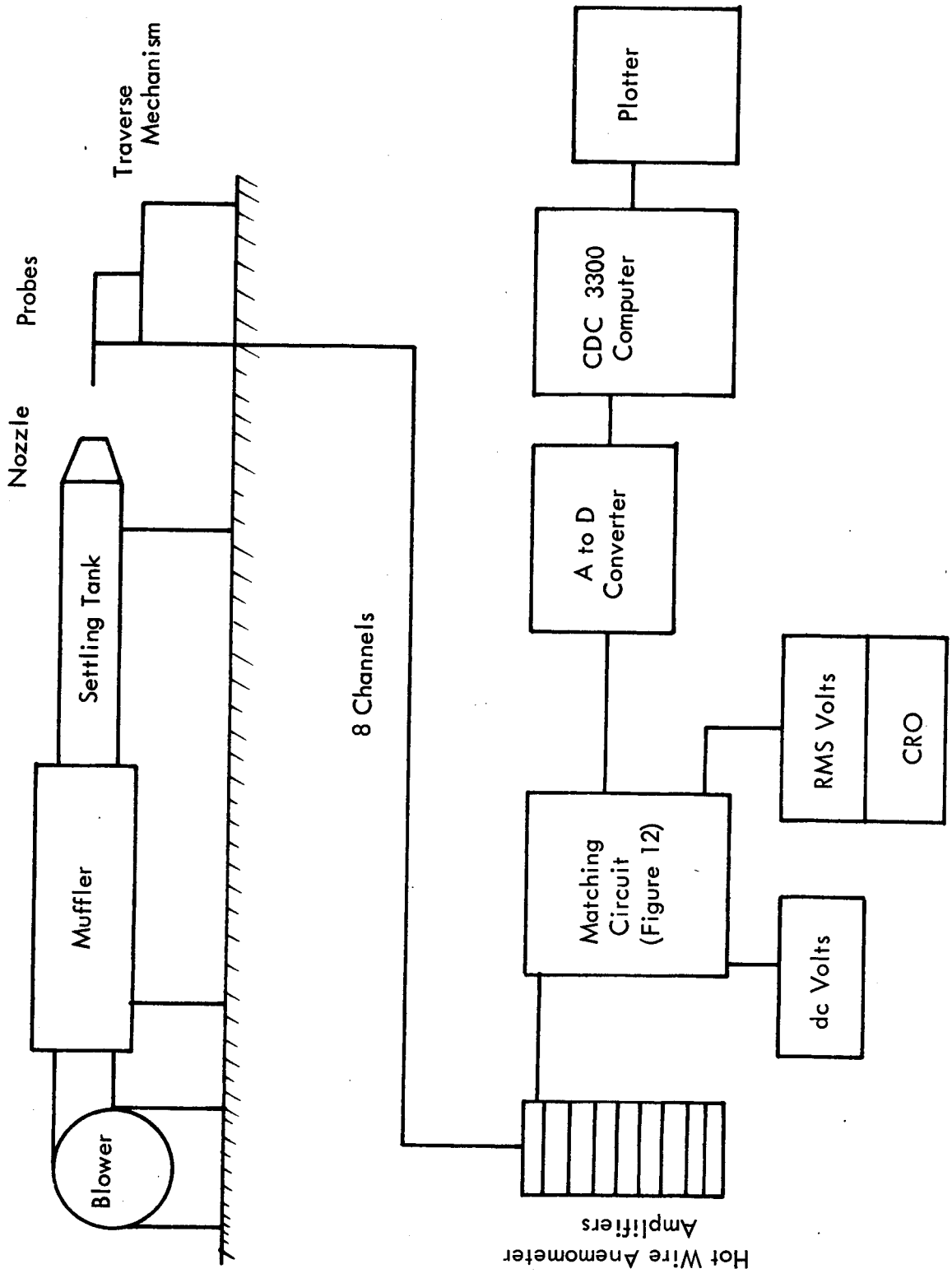

Figure 11. Rig and Data Acquisition System

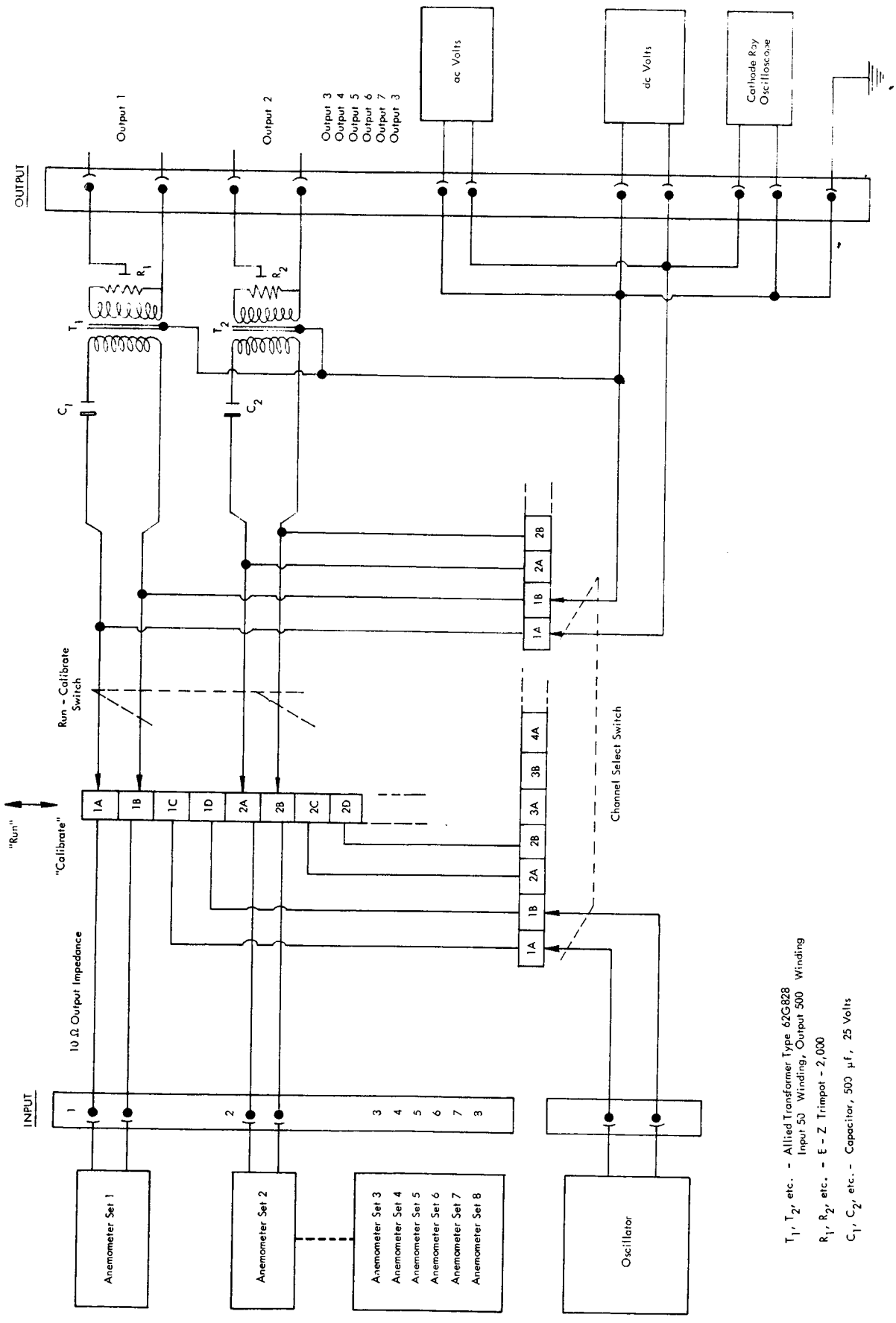

Figure 12. Multi-Channel Impedance Matching Circuit for the Anemometer System-Computer Interface

Figure 13. Reduced Horizontal Velocity Profiles of the Cold Air Jets

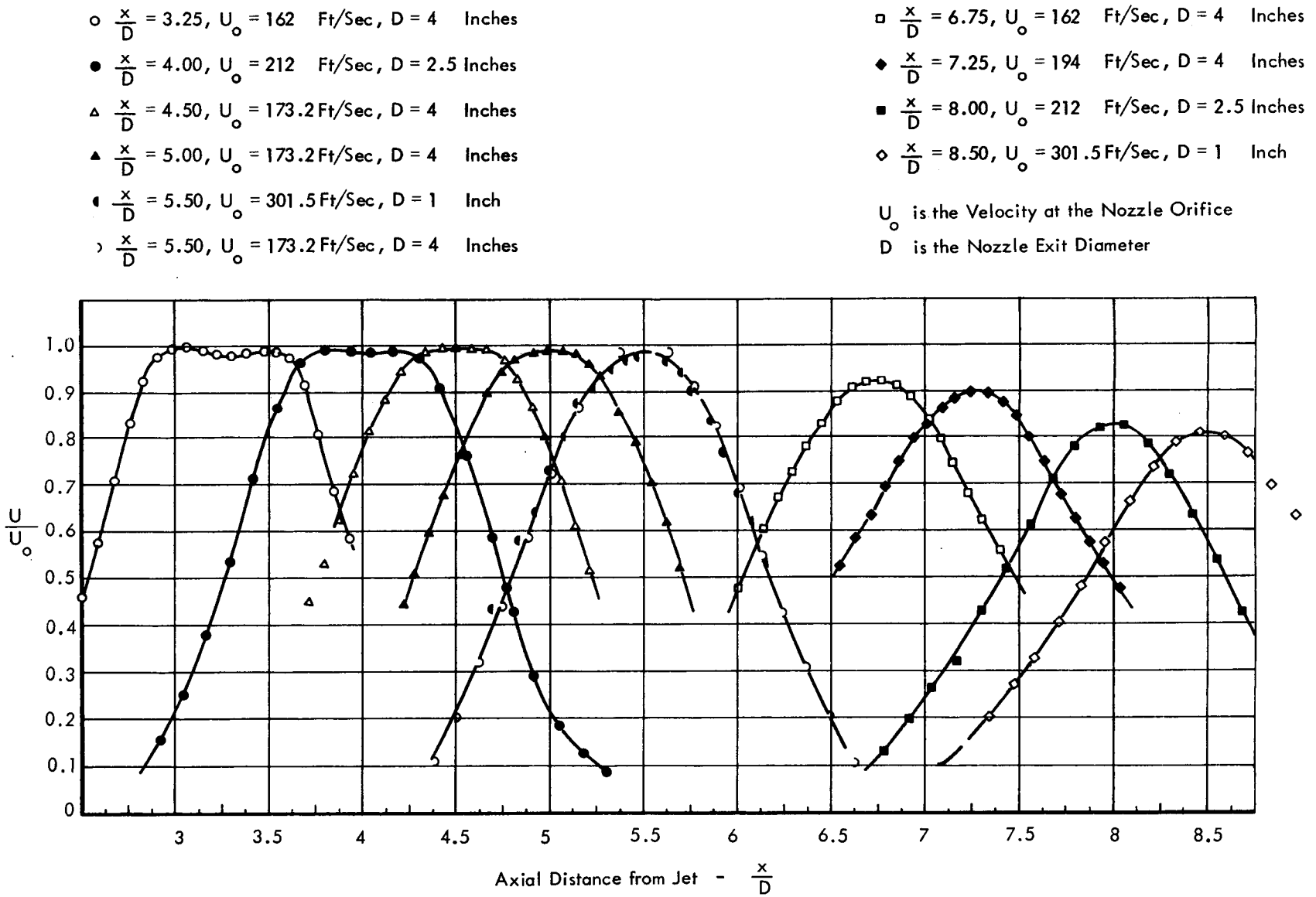

The upper side of the abcissa is marked off in intervals corresponding to an increment in y/D of 0.100, where y/D is the reduced horizontal distance across the jet. Each profile is thus centered on its axial distance from the jet, $\frac{x}{D}$.

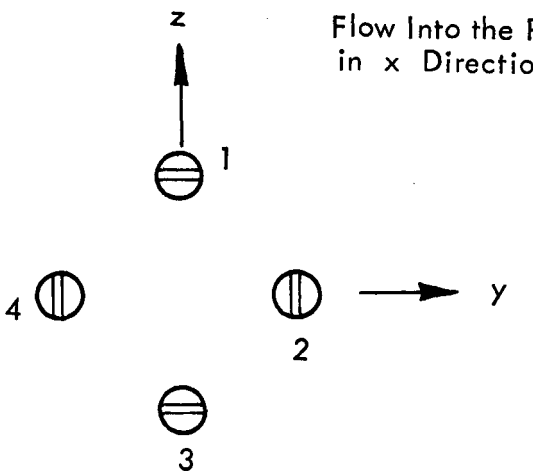

Square Array

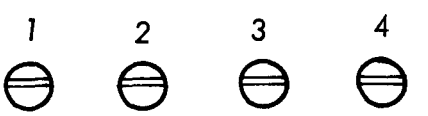

Line Array 1, u and v Measurements

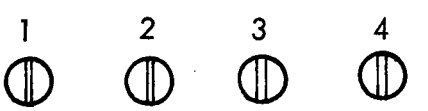

Line Array 2, u and w Measurements

Figure 14. Probe Arrays

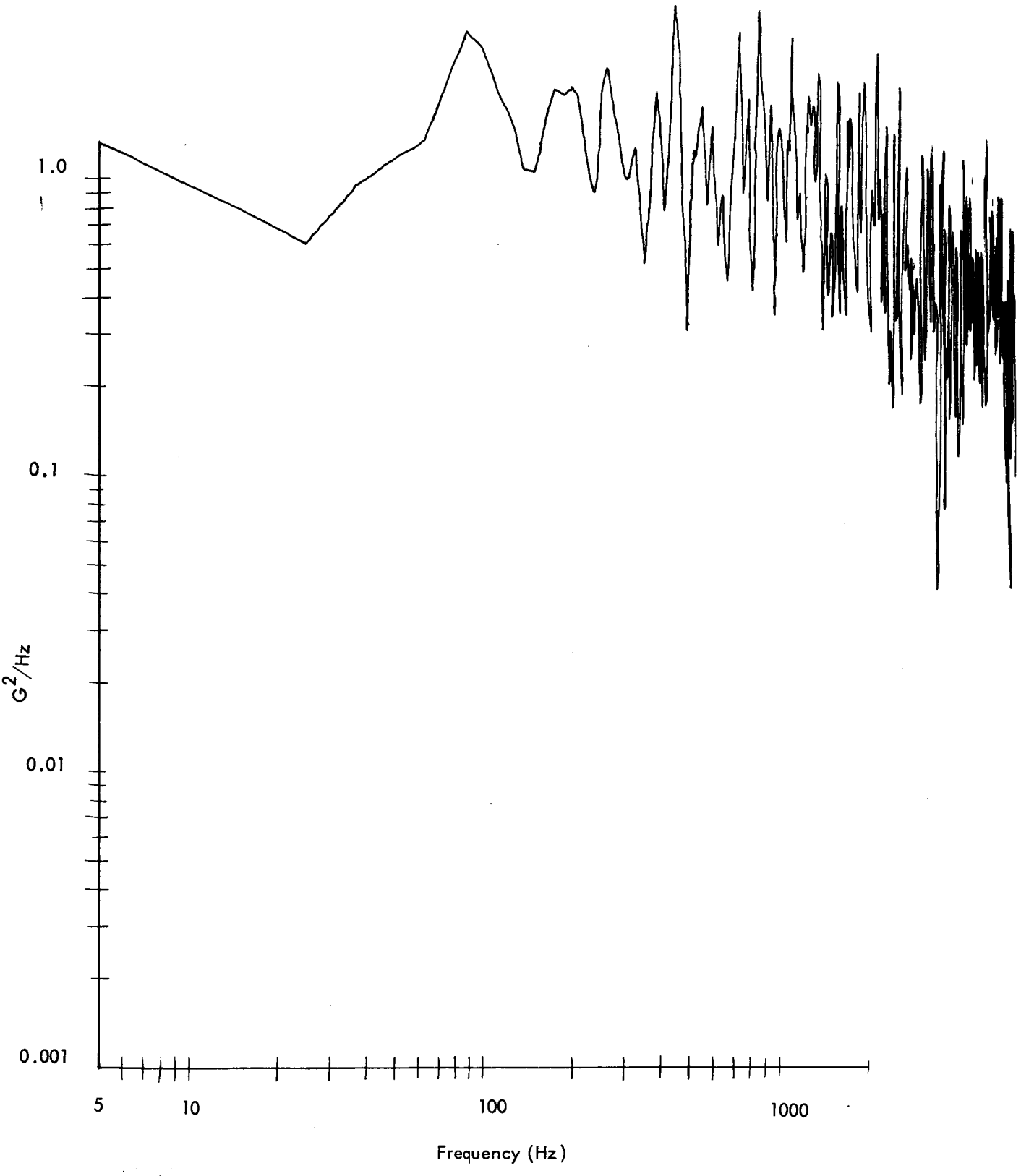

Figure 15. Spectra of Wire Output, No Damping

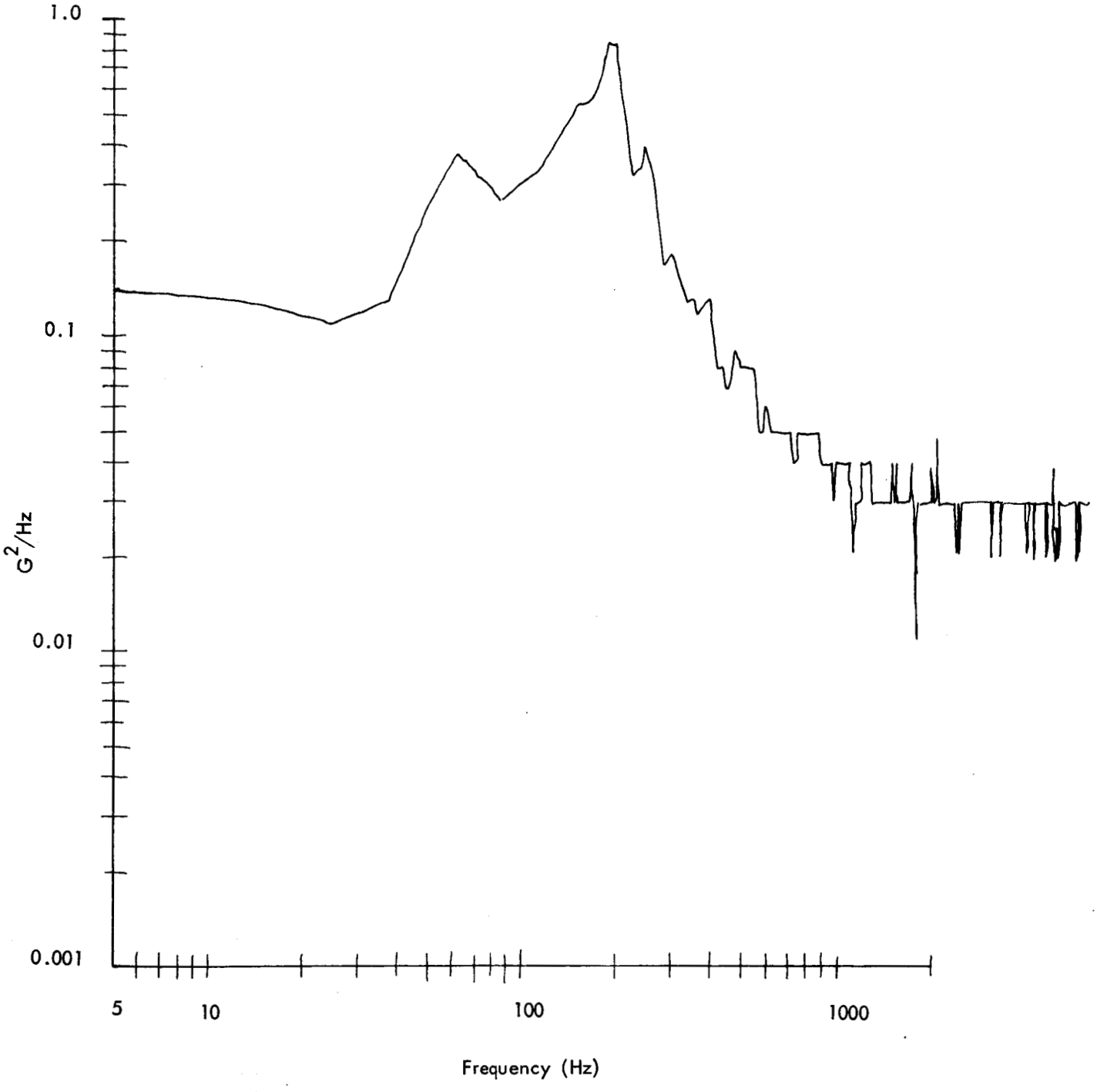

Figure 16. Spectra of Wire Output, Some Damping

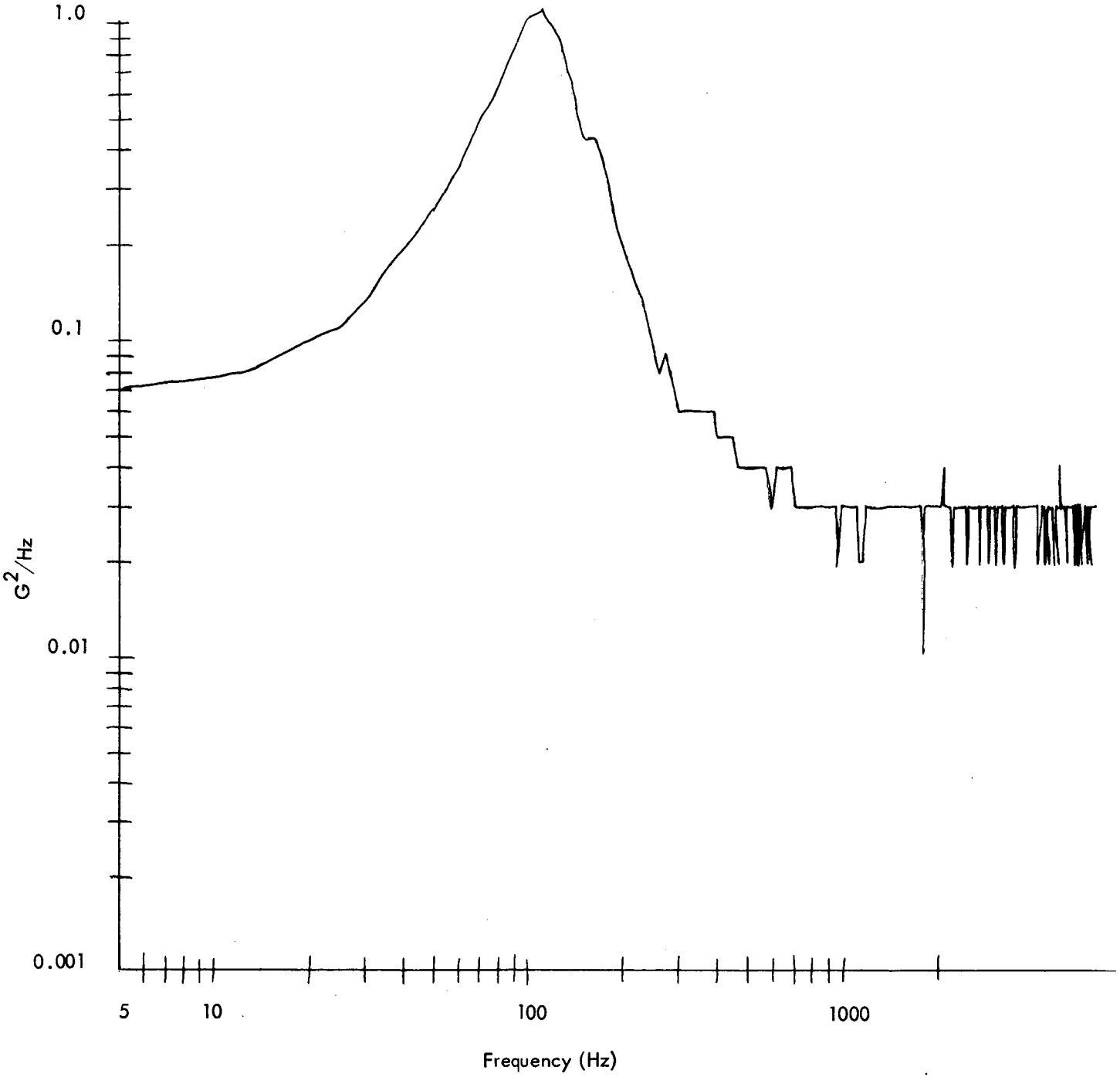

Figure 17. Spectra of Wire Output, Maximum Damping

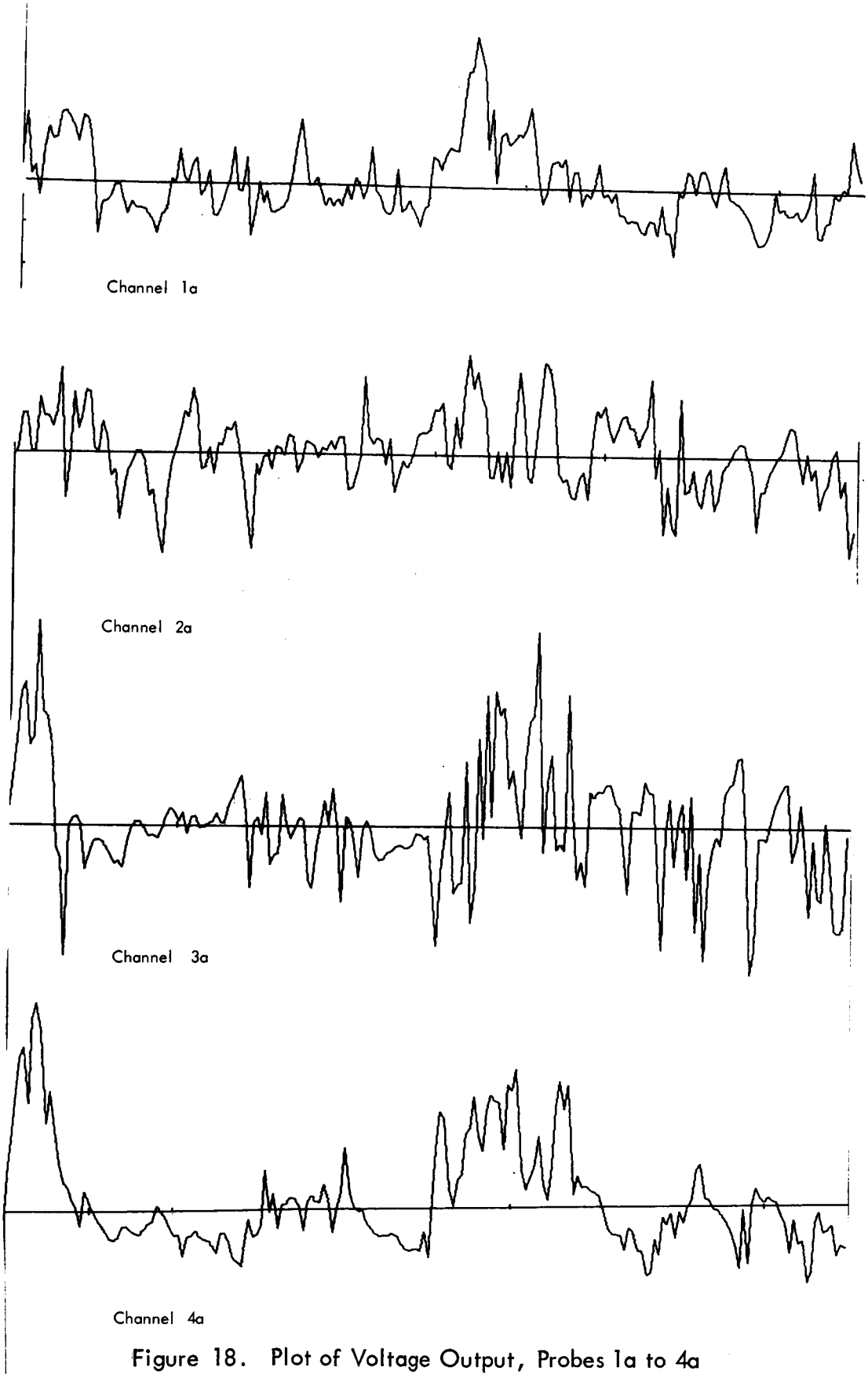

Figure 18. Plot of Voltage Output, Probes 1a to 4a

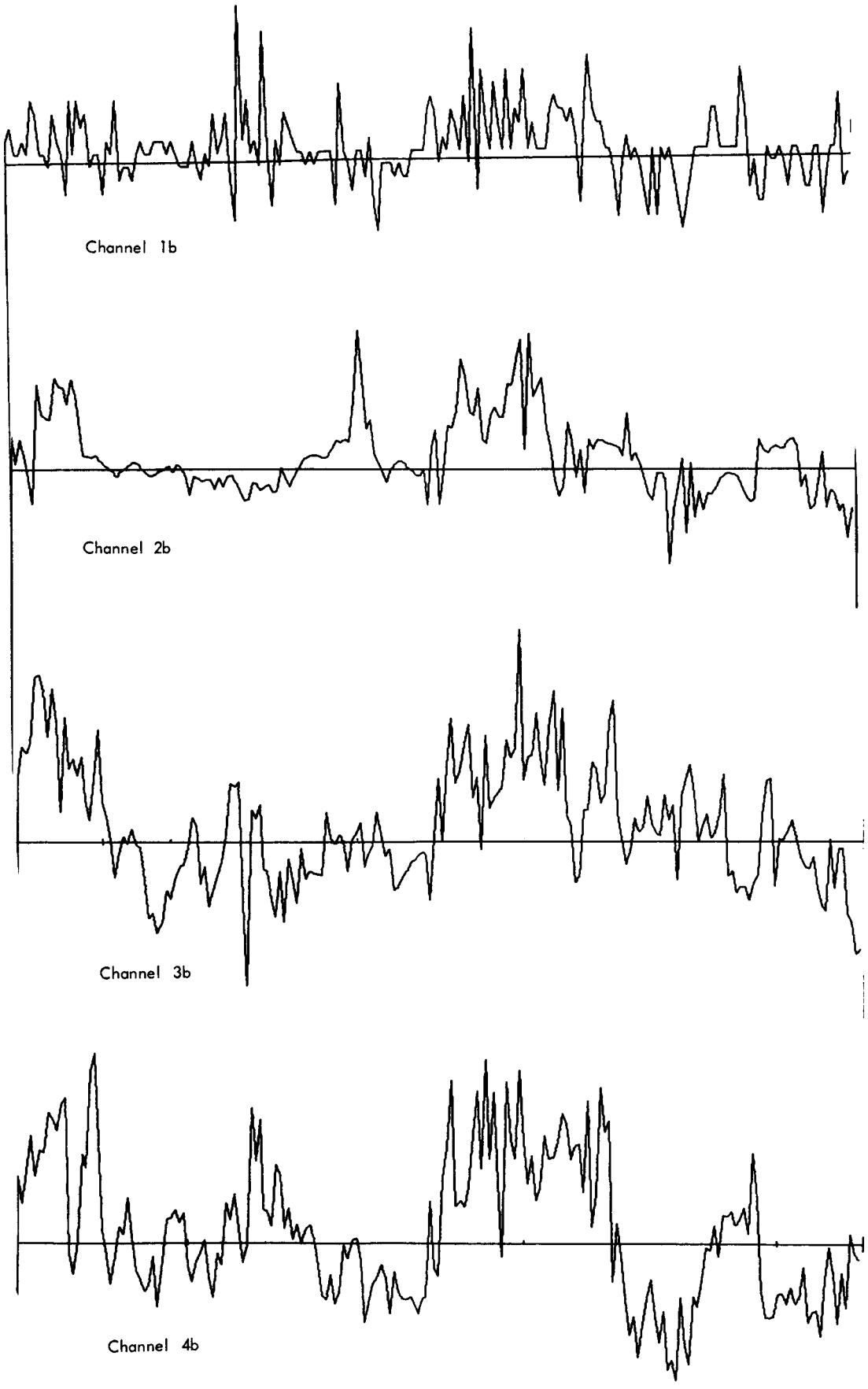

Figure 19. Plot of Voltage Output, Probes 1b to 4b

u	v	w	p	θ	φ
1.70902715E 02	7.88863607E 00	2.46962716E 00	1.71102506E 02	4.61258949E+02	1.44341131E-02
-3.84804366E 01	-2.13280099E 00	6.95404359E-01	3.85457706E 01	5.53689409E+02	1.80419817E-02
-5.68348318E 01	-2.49093973E 00	-4.69713416E-01	5.68913308E 01	4.37996660E+02	-8.25642056E-03
-1.47677656E 02	-6.72775610E 00	-1.54286797E 00	1.47838876E 02	4.55255567E+02	-1.04363346E-02
-1.16543093E 02	-5.09429101E 00	-1.82464115E 00	1.16668649E 02	4.36838427E+02	-1.56403246E-02
-2.40337266E 02	-1.25419013E 01	1.00117964E 00	2.40666373E 02	5.21372953E+02	4.16004330E-03
1.81316152E 02	9.31147784E 00	1.02357732E 00	1.81557975E 02	5.13038521E+02	5.63777350E-03
6.22401519E 01	5.18280026E 00	-4.34507336E 00	6.26065299E 01	8.30793373E+02	-6.94587152E-02
6.71203534E 01	3.94047884E 00	-3.47320759E-01	6.72368191E 01	5.86403514E+02	-5.15565639E-03
1.05223936E 02	6.03114020E 00	-8.97149091E-01	1.05400456E 02	5.72545451E+02	-8.51191691E-03
2.71620155E 02	1.42330017E 01	-7.72182106E-02	2.71992817E 02	5.23525073E+02	-2.83897981E-04
7.97771745E 01	2.42289506E 00	5.60205202E 00	8.00103180E 01	3.03614479E+02	7.03739539E-02
5.97751287E 02	3.02040520E 01	1.21539591E 00	5.98515131E 02	5.04865252E+02	2.03068675E-03
3.79343656E 02	1.76923713E 01	4.85972514E 00	3.79787107E 02	4.66056553E+02	1.27962684E-02
1.91451408E 02	9.74829504E 00	9.85395105E-01	1.91481987E 02	5.08792256E+02	5.14083357E-03
2.78716897E 02	1.31788790E 01	3.47993229E 00	2.79049908E 02	4.72489131E+02	1.24709640E-02
8.90757615E 01	3.92362999E 00	2.15704104E 00	8.91882224E 01	4.40197006E+02	2.41878505E-02
-1.98593186E 02	-1.17433793E 01	4.65394118E 00	1.98994522E 02	5.90640622E+02	2.33894154E-02
-1.65474385E 02	-1.12890102E 01	7.94955835E 00	1.66049419E 02	6.81165544E+02	4.78929602E-02
3.89519939E 01	-1.46069795E-01	5.91780764E 00	3.93991348E 01	-3.74998738E+03	1.50772043E-01
4.07304078E 01	1.55553617E 00	1.48508173E 00	4.07871460E 01	3.81724770E+02	3.64185829E-02
-1.24037651E 02	-6.45879063E 00	5.03964299E-01	1.24206718E 02	5.20242246E+02	4.05747522E-03
-1.02617402E 02	-4.98613084E 00	-6.50970452E-01	1.02740530E 02	4.85513403E+02	-6.33610523E-03
5.74509917E 01	3.02537952E 00	-5.33505165E-01	5.75330688E 01	5.26115828E+02	-9.27315060E-03
2.70043198E 01	8.34289832E-01	1.20303392E 00	2.70439756E 01	3.08848566E+02	4.44990435E-02
2.33029006E 02	1.10312677E 01	1.76758169E 00	2.33296659E 02	4.73032898E+02	7.57661343E-03
1.40372616E 02	6.87463995E 00	2.54672175E 00	1.40527073E 02	4.32481228E+02	1.81236335E-02
6.41862382E 01	2.42774632E 00	2.04605441E 00	6.42647140E 01	3.78054496E+02	3.18432948E-02
3.40119484E 01	1.77393408E 00	-2.60650875E-01	3.40591752E 01	5.21099869E+02	-7.65295746E-03
-4.03697391E 00	1.89612297E-01	-1.13375428E 00	4.19744088E 00	-4.69344248E+02	-2.73503200E-01
-2.10369912E 01	-2.40179852E-01	-2.37058598E 00	2.11725085E 01	1.14165289E+02	-1.12628333E-01
-1.78750324E 01	1.32019689E-01	-3.09049832E 00	1.81407109E 01	-7.38556920E+03	-1.71197617E-01
1.16747964E 02	6.51706864E 00	-1.99114423E 00	1.16946572E 02	5.57638165E+02	-1.70270809E-02
6.73146754E 01	4.55913375E 00	-3.51946978E 00	6.75606239E 01	6.76253977E+02	-5.21170963E-02
2.76708920E 02	1.46971268E 01	-2.23019693E 00	2.77107932E 02	5.30641711E+02	-8.04820342E-03
3.86944474E 02	1.95631677E 01	-2.25769582E-01	3.87438762E 02	5.05150635E+02	-5.82723303E-04
1.29870771E 02	6.81062179E 00	-8.74883984E-01	1.30052171E 02	5.23935348E+02	-6.72722784E-03
2.36803126E 01	1.39259983E 00	-6.76627128E-01	2.37308736E 01	5.87406840E+02	-2.85163897E-02
-7.43725220E 01	-3.51558071E 00	-8.85754441E-01	7.44608347E 01	4.72347269E+02	-1.18958555E-02
-9.60945682E 01	-4.80143395E 00	-3.00449408E-01	9.62149161E 01	4.99241976E+02	-3.12269562E-03
-2.11190039E 02	-1.04301434E 01	-8.72542861E-01	2.11458230E 02	4.93452830E+02	-4.12632479E-03
-2.19751377E 02	-1.08669606E 01	-8.66953922E-01	2.20021613E 02	4.94109097E+02	-3.94032274E-03
-4.39827312E 02	-2.26651374E 01	6.06408432E-01	4.40411331E 02	5.14863584E+02	1.37691422E-03
-2.76397422E 02	-1.35538522E 01	-1.48962198E 00	2.76733556E 02	4.89982995E+02	-5.38290044E-03
-1.62870722E 01	-6.34868115E-01	-8.33297569E-01	1.63207281E 01	3.89601552E+02	-5.10798319E-02
-5.79066736E 01	-2.19672256E 00	-2.41415797E 00	5.79985913E 01	3.79173860E+02	-4.16364533E-02
-1.25368427E 02	-5.56060061E 00	-2.48903464E 00	1.25516366E 02	4.43250235E+02	-1.98316593E-02
-4.47410721E 00	3.08845792E-02	-1.05579016E 00	4.59709496E 00	-6.90284949E+03	-2.31733099E-01
-1.83859282E 02	-9.85089754E 00	-1.13244443E 00	1.84079114E 02	4.91892841E+02	-6.15198299E-03
-1.09086158E 02	-5.98336770E 00	9.67464985E-01	1.09254412E 02	5.47950194E+02	8.85527284E-03
-2.22464256E 02	-1.22069046E 01	2.23973771E 00	2.22810166E 02	5.48163368E+02	1.00523934E-02
-1.50690715E 02	-8.63163228E 00	2.54176096E 00	1.50959124E 02	5.72179286E+02	1.48382077E-02
-1.86616631E 02	-9.87816232E 00	1.05206052E 00	1.86888849E 02	5.28835609E+02	5.62960881E-03
-1.44538035E 02	-6.40332905E 00	-2.87987555E 00	1.44708465E 02	4.42730856E+02	-1.09025378E-02
-8.74945631E 01	-2.96361036E 00	-4.63581679E 00	8.76673962E 01	3.38589924E+02	-5.29042746E-02
8.42138095E 01	2.97970599E 00	2.95081748E 00	8.43181575E 01	3.53678746E+02	3.50033756E-02
2.30499898E 02	1.04357228E 01	2.76512710E 00	2.30752580E 02	4.52434095E+02	1.19833688E-02
-1.16121947E 01	-3.99071465E 00	6.42225232E 00	1.36258104E 01	2.60130341E+01	4.90829485E-01
-1.43257601E 01	-8.65217169E-01	1.74324271E-03	1.43518642E 01	6.03226252E+02	1.21465942E-04
-1.27843460E 02	-6.60067318E 00	-1.19800112E-01	1.28013802E 02	5.15850971E+02	-9.35837599E-04
-1.17104899E 02	-5.90612419E 00	-5.45523590E-01	1.17257007E 02	5.03909194E+02	-4.65239197E-03
-5.00489189E 01	-2.29855376E 00	-1.08092336E 00	5.01133318E 01	4.58938935E+02	-2.15712498E-02
-1.77216742E 02	-9.74053114E 00	1.62329595E 00	1.77491652E 02	5.49086952E+02	9.14588694E-03
-1.66501219E 02	-8.36197072E 00	-7.39753443E-01	1.66712704E 02	5.01795192E+02	-4.43730954E-03
-7.14864072E 00	-7.76718603E-01	9.65935077E-01	7.25530058E 00	1.08228069E+01	1.33531540E-01
-1.75440914E 02	-8.23555183E 00	-2.04328022E 00	1.75645990E 02	4.69075910E+02	-1.16332079E-02
-2.09052498E 02	-1.02293081E 01	-1.40657801E 00	2.09307344E 02	4.88927701E+02	-6.72020641E-03
1.46304624E 01	6.93831528E-01	-1.14439918E-01	1.46473522E 01	4.73882552E+02	-7.81309008E-03
1.89366822E 00	3.65174488E-01	-9.05716930E-01	2.13064659E 00	1.90501311E+01	-4.39061506E-01
-4.56817661E 01	-1.94599444E 00	-1.04012046E 00	4.57350248E 01	4.25731922E+02	-2.27442784E-02
-1.43030869E 01	-2.85821319E-01	-1.20008158E 00	1.43561897E 01	1.99805318E+02	-8.36909851E-02
1.68371225E 01	6.03255376E-01	5.88565612E-01	1.68582034E 01	3.58135684E+02	3.49198092E-02
6.36574503E 01	3.34492323E 00	-3.83513777E-01	6.37464240E 01	5.24973874E+02	-6.01627616E-03
9.46597037E 00	6.84718200E-01	-4.69673455E-01	9.50231694E 00	7.22089431E+02	-4.94474040E-02
9.51544507E 00	9.10847946E-01	-1.13594223E 00	9.62620117E 00	9.54323342E+02	-1.18282943E-01
-3.71388504E 01	-7.53533790E-01	-2.97730560E 00	3.72656192E 01	2.02868534E+02	-7.99794071E-02
4.98871200E 01	3.27751051E 00	-1.85890709E 00	5.00292150E 01	6.56042505E+02	-3.71649843E-02
3.89580148E 01	2.75081325E 00	-1.83009051E 00	3.90978659E 01	7.04926904E+02	-4.68250480E-02
3.74684734E 01	2.35613568E 00	-1.11003988E 00	3.75590874E 01	6.28001269E+02	-2.95587997E-02
3.00961276E 02	1.43684912E 01	2.50636316E 00	3.01314495E 02	4.77057699E+02	8.31819278E-03
2.57876541E 02	1.33410658E 01	-5.37490099E-01	2.58221965E 02	5.16882329E+02	-2.08150568E-03
4.21348314E 02	2.21040431E 01	-1.25655117E 00	4.21929579E 02	5.24122166E+02	-2.97811078E-03

Figure 20. Calculated Values of the Fluctuating Velocity Components

Figure 21. Isometric Plot of the Fluctuating Velocity Vector